# DESIGNING A ROBUST CONTROLLER TO DAMP SUB-SYNCHRONOUS OSCILLATIONS IN POWER SYSTEMS

Chamali Mahawala Gamage

(168660P)

Degree of Master of Science

Department of Electrical Engineering

University of Moratuwa

Sri Lanka

July 2020

# DESIGNING A ROBUST CONTROLLER TO DAMP SUB-SYNCHRONOUS OSCILLATIONS IN POWER SYSTEMS

Chamali Mahawala Gamage

(168660P)

Thesis/Dissertation submitted in partial fulfillment of the requirements for the degree Master of Science

Department of Electrical Engineering

University of Moratuwa

Sri Lanka

July 2020

# DECLARATION

I declare that this is my own work and this thesis/dissertation2 does not incorporate without acknowledgement any material previously submitted for a Degree or Diploma in any other University or institute of higher learning and to the best of my knowledge and belief it does not contain any material previously published or written by another person except where the acknowledgement is made in the text.

Also, I hereby grant to University of Moratuwa the non-exclusive right to reproduce and distribute my thesis/dissertation, in whole or in part in print, electronic or other medium. I retain the right to use this content in whole or part in future works (such as articles or books).

Signature: Date: ……..

……

C.M. Gamage

The above candidate has carried out research for the Masters thesis/ dissertation under my supervision.

Signature of the supervisor:

…… Date: ……..

Dr. W. D. Prasad

## ABSTRACT

In the power transmission systems, the power transferring capability is limited due to the inductive reactance of the transmission lines. In order to mitigate the inductive effect, some compensation techniques are applied to the transmission lines. One such technique is the series compensation using capacitor banks. Series compensation method is used to improve the system voltage with capacitor banks are connected in series with the power transmission line and it expands the power transferring capability of the line. Although the increase of series compensation improves the power transfer capability and the steady-state and transient stability limit of the power transmission line, it can lead to the generation of some natural frequencies due to the combination of inductor and capacitor (L-C). These frequencies are called as sub-synchronous frequencies which are below the power frequency of the power systems. They can arise sub-synchronous resonance (SSR).

The SSR can cause physical damages to the power system equipment unless it is detected and mitigated punctually. Several number of mitigation techniques for different types of power system oscillations have been proposed in literature. But existing mechanisms are not completely damp these oscillations or the mechanisms used to damp these oscillations might be source for any other control situations. Therefore, this is a phenomenon which should understand well and damped these oscillations properly. The intension of the work presented in this thesis is to properly mitigate the undamped power system oscillations which are in the range of sub-synchronous frequencies.

This research proposed a robust controller which can damp dominant sub-synchronous resonance. Further, the implemented controller performs well in different operating points. IEEE First Benchmark Model (FBM) is used as the test system and the dynamic phasor representation of the system is used to model the small signal model. The operating points of the test system were generated by changing the series capacitor compensation level of the power transmission line. Finally, this research introduced a robust controller with PID controlling to damp out dominant sub-synchronous oscillations which can perform well under different operating points of the selected power system.

# ACKNOWLEDGEMENT

First, my sincere thanks must go to my advisor, Dr. W. D. Prasad for his continuous advice, guidance, encouragement and patience throughout the course of this work. It has been a privilege to work under his guidance. I am also thankful to the course coordinator, Dr. Buddhika Jayasekara and the staff of the Department of Electrical Engineering, University of Moratuwa for their continuous encouragement.

Further, I am thankful to my father and late mother for believed that I can always do better than I believed in myself. A special thank goes to my husband for encouraged me to reach for a successful end.

C.M. Gamage
July 2020
University of Moratuwa.

# TABLE OF CONTENT

# LIST OF FIGURES

# LIST OF TABLES

# LIST OF ABBREVIATIONS

| | |
|---|---|
| AC | Alternating Current |
| SSR | Sub-Synchronous Resonance |
| PSS | Power System Stabilizer |
| AVR | Automatic Voltage Regulator |
| FACTS | Flexible AC Transmission Systems |
| HVDC | High-Voltage Direct Current |
| SVC | Static Var Compensators |
| STATCOM | Static Synchronous Compensator |
| SSDC | Sub-Synchronous Damping Controller |
| TCSC | Thyristor Controlled Series Compensation |
| IEEE | Institute of Electrical and Electronics Engineers |
| FBM | First Benchmark Model |
| SSSC | Static Synchronous Series Compensator |
| FLC | Fuzzy Logic Control |
| FFT | Fast Fourier Transform |
| HP | High Pressure |
| IP | Intermediate Pressure |
| LPA | Low Pressure A |
| LPB | Low Pressure B |
| SA | Simulated Annealing |
| VSC | Voltage Sourced Converter |

# CHAPTER 01

# INTRODUCTION

It is well known that most AC transmission systems use capacitors in series with the transmission lines. Series capacitor compensation is used for several reasons such as increasing the load capability, controlling the load sharing among parallel lines and also enhancing transient stability. However, series compensation capacitors in power transmission lines can lead to SSR which is a form of oscillation occurs in the power system and leads to several problems such as shaft failures. Therefore, the SSR effects should be studied and understood for the series capacitor compensated power systems. [1]

This introductory chapter describes the nature of power system oscillations, several types of power system oscillations, problems with those power system oscillations and the motivation for the research.

## 1.1. Power System Oscillations

Due to the interactions among the components, the power systems contain with several modes of oscillations. Among these, swinging of the synchronous generator rotors with respect to another rotor in the same power system leads to a major type of power system oscillations. These electromechanical oscillation modes typically occur between the frequencies 0.1 Hz and 2 Hz [2]. The interarea oscillation modes which are particularly troublesome, typically occur between the frequencies 0.1 Hz and 1 Hz [2]. The interarea oscillation modes are generally connected with the machine groups which are swinging with respect to other machine groups over a comparatively feeble path of transmission. The local mode of oscillations which are between the frequencies 1 Hz and 2 Hz, usually involve with the swinging of one or more generator rotors relative to the remainder of the

system or the swinging of the machines which are electrically closed, with respect to each other [2]. All of these oscillations are electromechanical low frequency oscillation modes. Other than these, sub-synchronous oscillations such as torsional modes of oscillations which the frequencies are below the synchronous frequency, typically occur between the frequencies 10 Hz and 45 Hz. The next sub sections discuss the several types of power system oscillations in detail.

### 1.1.1. Electromechanical Local Mode of Oscillations

Oscillations with electromechanical local mode is the most commonly encountered among the low frequency power system oscillations. This mode of oscillations occurs with the swing of a one synchronous generator or more in a power station, against the remain of that power station or load canter. This type of oscillations can become a sincere problem, in the power station with reactance tie-lines and high load. From the AVRs action in the generator units which are operating at high output and delivering to the feeble transmission networks, this type of oscillation problems can be caused. With the high response excitation systems, the problem is more noticeable. The electromechanical local mode of oscillations normally occur between the frequencies 1 Hz and 2 Hz. The appearance of these oscillations is properly understood and a satisfactory damping can be gladly reached by Power System Stabilizers (PSSs) form with the help of extra control of the excitation systems. [3], [4]

### 1.1.2. Electromechanical Inter-area Mode of Oscillations

Along with the local mode of oscillations, the inter-area mode of oscillations are also stated to be an effective power oscillation mode by the most authors. Large inter-area power oscillations can be produced by the local mode of oscillations and this is discussed in the reference [5]. This mode of oscillations is related with the oscillations between the

machines which are in two separate parts of the power system. These oscillations are caused by more than one groups of thoroughly coupled machines which are interconnected from the weak ties. The electromechanical inter-area mode of oscillations normally occur between the frequencies 0.1 Hz to 1 Hz. The characteristics of the inter-area mode of oscillations are complicated and pointedly different from the characteristics of the local mode of oscillations. The impact of these inter-area mode of oscillations is related to the location of the generator in the power system and the connection of PSS. Therefore, to damp this mode of oscillations and assurance the stability of the widespread power system network which has many generators, it's required to use a monitoring system and a reliable control such as PSSs. [3], [4]

### 1.1.3. Electromechanical Torsional Mode of Oscillations

Torsional mode of oscillations typically happens in the turbo machines (i.e. in steam driven systems). The long steam turbine-generator rotational components (such as shafts) have some mechanical torsional mode of oscillations on frequency in the sub-synchronous range which are originated by the variations in mechanical or electrical torques in the grid connected generators in the power transmission lines with a long series capacitor compensation. Due to the control interactions with the excitation of generator unit and control of the prime mover, there can be several instances of torsional mode instability. These oscillations typically occur around the frequencies higher than 10 Hz for the turbines with a speed of 3600 rpm and around 5 Hz for the turbines with a speed of 1800 rpm. Since, this mode contains the frequencies which are greater than the frequency range of typical PSS, monitoring this oscillation mode is difficult for the generator operators. When commerce with this oscillation mode, the excitation system which includes high gains can mains to shaft damages. [3] Flexible AC Transmission Systems (FACTS) were presented as a solution to control this mode of oscillations. More about these sub-synchronous oscillations and the defects of the existing solutions are discussed in the later sections.

### 1.1.4. Electromechanical Control Mode of Oscillations

Even though, the torsional mode of oscillations is damped, there are some elements which can affect for this damping of torsional mode of oscillations. For example, the damping can be affected by the unbalanced faults, control of the static VAR converter, control of the HVDC converter, control of the governor, and transmission with capacitors which are in series. These oscillations can be termed as the control mode of oscillations [6]. Oscillations in the control mode are related with the generating unit controlling as well as the controlling of other equipment. Controls which are not tuned well at the prime movers, excitation systems, high-voltage direct current (HVDC) converters, and static var compensators (SVC) are typical reasons of instability of the control mode. Sometimes, tuning of the controls is hard to guarantee an acceptable damping of all modes [3].

## 1.2. Problems with Power System Oscillations

The power system oscillations themselves can be activated by some events such as a disturbance occur at the power systems or fluctuating of the operating point of the system across some boundaries of steady state stability. When undamped oscillations start, they raise in magnitude concluded the extent of several seconds [2]. In some cases, the power system oscillations cause large generators to lose synchronism of the electrical network. Through slow cascading outages, the same effect can be reached when, the power system oscillations are persistent and sturdy enough to lead to automatic uncoordinated disconnection of the main loads or generators. When the continued oscillations don’t produce disconnections in the networks or loss of resources, they can interrupt the power system in other ways. As an example, the unacceptable voltage or frequency swings can be associated with the power swings which can limit the power transfers even when, the stability is not a direct concern [2].

The local mode or inter-area mode of oscillations which are not damped well, cause pressures to the safe system operation. The inter-area mode of oscillations earn relatively more attention, since these oscillations comprise with generating units in two or more areas and presents of individual units may lead for larger oscillations in the tie lines. Inter-area connections with bulk power can be affected significantly by this factor. The poorly damped torsional mode of oscillations may result in the interruption in the generator, because of the process of protective devices which are used to ward off the serious damage occur to the shaft of turbine-generator unit. Hence, by means of wide-ranging power system analysis, an adequate damping of the torsional mode of oscillations should be guaranteed in the all possible operating points. [5]

The power system oscillations which are not properly controlled, that can lead to interruptions in the power system or partial or full blackout of the system. Hence a comprehensive understanding of this problem will help to find effective remedial ways, means and measures to control them. There are number of mechanisms to mitigate the damping of oscillations in power systems. The existing mechanisms to reduce the damping of SSR and their defects are discussed in the later sections.

## 1.3. Motivation for the Research

As described in the section 1.2, power system oscillations can cause physical damages to the power system equipment unless they are detected and mitigated punctually. Several mitigation approaches for these different types of oscillations in power systems have been proposed in literature. But existing mechanisms are not completely damp these oscillations or the mechanisms used to damp these oscillations might be source for any other control situations. This thesis mainly considers the Sub-Synchronous Resonance (SSR) which is a risk situation. The SSR is a hazard situation from the oscillations in power systems which are belong to the range of sub-synchronous frequencies. SSR can lead to huge damages to the power system networks such as shaft stress and fatigues, possible damages and other

failures. Therefore, this is a phenomenon which should understand well and damped these oscillations properly. The motivation of this thesis is to mitigate the undamped oscillations in power systems properly which are in the sub-synchronous frequency range. Some incidents cause by SSR phenomena are discussed below with the main incident and the damage occurs in 1970 and 1971 at the power station, Mohave in southern Nevada.

In 1970 and also in 1971, the generator at Mohave power station experienced a vibration which was increased gradually. As a result of this vibration, the shaft between generator and rotating exciter was fractured. From the analysis of this incident, found that an electrical resonance produced a torque at 29.5 Hz with the resonance frequency at 30.5 Hz and the system frequency at 60 Hz. This electrical resonance was nearly equivalent with the frequency of the second turbine-generator torsional mode of vibration which was at the frequency, 30.1 Hz. This interface between the torsional system and series capacitors came to be recognized as SSR. [6]

After this incident, many researches were done on SSR and the methods to mitigate these resonances. This research also states a method to mitigate the SSR in a better way than the existing researches by implementing a robust controller.

## 1.4. Thesis Outline

The remain of the thesis is ordered as mentioned below.

Chapter 2 presents a detailed description on sub-synchronous oscillations in power systems, SSR in series capacitor compensated transmission lines and the types of sub-synchronous oscillations in series capacitor compensated lines and a comprehensive literature review on proposed techniques to damp SSR. Conventional solutions to sub-synchronous resonance problems and the FACTS devices are include for the literature review. Finally, the defects of the existing methods and the objectives of the research are discussed.

Chapter 3 presents the methodology proposed for this research.

Chapter 4 presents the detailed development of the linearized state space representation for the selected IEEE benchmark model. First, it is discussed why the test system was selected. The conventional generator model, the generator model including the stator transients, the network model the combination of the generator and network model, the multi-mass turbine model, overall state space model, inceptive conditions of the test system state variables and the eigenvalue analysis for the test system are indicated. Finally, the model verification is also presented.

Chapter 5 presents the designing of the controller. First, the Ziegler Nichols (Z-N) method to select the inceptive values for the P, I and D controller parameters and then, Simulated Annealing Method to optimize the parameter values. Then simulation results obtain with and without the PID controller are presented.

# CHAPTER 02

# SUB-SYNCHRONOUS OSCILLATIONS IN THE POWER SYSTEMS

In thermal power stations, sub-synchronous oscillation incident is an anomalous state which the steam turbine unit, after disturbance is under particular operation state. On the proceeding condition, significant energy exchange can be occurred between steam turbine-generator set and electrical system at the synchronous frequency. There was a severe damage on large-scale turbo- generator rotor shaft at Mohave Generating Station in year 1970 and 1971 caused by series capacitor compensated transmission [7]. After this damage, people in industry and academic started to study about sub-synchronous oscillation problem fervently and achieved remarkable results in mechanism investigation methods and the limiting methods.

AC transmission lines with series capacitor compensation and high voltage DC transmission are generally applied to solve the problems with large-scale wind power transmission systems because, the wind power station is distant from the load center. Series capacitor compensation can induce problem of wind turbine with sub-synchronous oscillation, affect the stable and safe operation of wind farms and also the power transmission system. This chapter discuss about the sub-synchronous oscillations occur in the power systems due to the series capacitor compensation and the sub-synchronous resonance which is a special incident of the sub-synchronous oscillations. Then, discuss about the existing solutions to mitigate sub-synchronous oscillations, their defects and the objectives of this thesis.

## 2.1. SSR in Series Capacitor Compensated Transmission Line

In the power transmission systems, the capability of power transferring is limited because of the inductive reactance of the power transmission line. To mitigate the inductive effect,

some compensation techniques are applied to the transmission lines. One such technique is the series compensation using capacitor banks. Series compensation method is applied to increase the system power by using a capacitor connected in series with the power transmission line. The phenomenon is also can state as, inserting reactive power in series with the power transmission line to improve the system impedance. This series compensation phenomenon increases the power transferring capability of the transmission line.

Although the increase of series compensation leads to the enhancement of the capability of power transferring and the steady-state and transient stability limit of the transmission line, it may also lead to the generation of some natural frequencies due to the combination of inductor and capacitor (L-C). These frequencies are under the power frequency, which are called as sub-synchronous frequencies as described in the section 1.1.3. If these frequencies match with the turbine-generator unit's natural torsional mode frequencies, it may lead to fatal effects. Frequencies which are in sub-synchronous range and SSR can be described by considering a RLC series connected branch as shown in Figure 2.1.

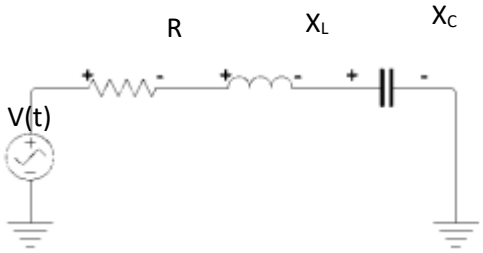


*Figure 0.1: RLC series connected branch*

Where,

$$X_L = \omega_1 L = 2\pi f_1 L$$

$$X_C = \frac{1}{\omega_1 C} = \frac{1}{2\pi f_1 C}$$

$$Z(j\omega_1) = R + j\omega_1 L + (j\omega_1 C)^{-1}$$

$$v(t) = \sqrt{2}Vsin(\omega_1 t + \theta)$$

Laplace transform should be applied to the voltage and impedance equation and equations 2.1 and 2.2 give these two equations in Laplace domain.

$$Z(s) = R + sL + \frac{1}{sC} \quad 0.1$$

$$V(s) = \sqrt{2}V\frac{s.sin\theta + \omega_1.cos\theta}{s^2 + {\omega_1}^2} \quad 0.2$$

Then, the branch current is given by the equation 2.3 and that equation can solve further as given in equation 2.4.

$$I(s) = \frac{V(s)}{Z(s)} = \frac{{sV(s)}/{L}}{s^2 + {R}/{L}\, s + {1}/{LC}} \quad 0.3$$

$$I(s) = \frac{{sV(s)}/{L}}{s^2 + 2\xi\omega_n s + {\omega_n}^2} = \frac{{sV(s)}/{L}}{(s-a)^2 + {\omega_2}^2} \quad 0.4$$

By considering voltage and current equations, some important terms can be defined as follows,

- Undamped natural frequency, $\omega_n = \sqrt{\frac{1}{LC}}$

- Damping ratio, $\xi = \frac{R}{2}\sqrt{\frac{C}{L}}$
- Damping rate, $a = -\xi\omega_n$
- Damping frequency, $\omega_2 = \omega_n\sqrt{1-\xi^2}$

Inverse Laplace transform of the current can be given as in the equation 2.5.

$$i(t) = K[A.sin(\omega_1 t + \psi_1) + B.e^{-\xi\omega_2 t}\sin(\omega_2 t + \psi_2)] \quad 0.5$$

Where,

$$K = \frac{\sqrt{2}\omega_2 CV cos\theta}{[({\omega_2}^2 - {\omega_1}^2) + 4\xi^2{\omega_1}^2{\omega_2}^2]^2}$$

$$B = \omega_1\sqrt{\frac{1 - 2a\xi\omega_2 + a^2{\omega_2}^2}{1-\xi^2}}$$

$$A = \omega_2\sqrt{1 + a^2{\omega_2}^2}$$

$$d = \sqrt{1-\xi^2}$$

$$\psi_1 = \theta + tan^{-1}\left(\frac{2\xi\omega_1\omega_2}{{\omega_2}^2 - {\omega_1}^2}\right)$$

$$\psi_2 = tan^{-1}\left(\frac{ad\omega_2}{1 - a\xi\omega_2}\right) - tan^{-1}\left(\frac{-2d\xi{\omega_2}^2}{2\xi{\omega_2}^2 + {\omega_1}^2 - {\omega_2}^2}\right)$$

In equation 2.5, the current response $i(t)$, has two different frequencies $\omega_1$and $\omega_2$. $\omega_1$is a sinusoidal component at the dynamic voltage frequency and $\omega_2$ is a damped sinusoidal component at a frequency which is depending on the network elements R, L and C and it's given by equation 2.6.

$$\omega_2 = d\omega_n = \omega_n\sqrt{1-\xi^2} = \frac{1}{2L}\sqrt{\frac{4L - R^2C}{C}} \qquad 0.6$$

For a 3-phase network other two phases, phase B and C will have the two frequencies present in their current responses with two different coefficients on the transient component of the current response. When these types of currents flow in the generator stator windings, Park's transformation can be used to describe the physical process of reflecting of currents into the generator mathematically. The Park's transformation matrix can be defined as shown in the equation 2.7.

$$P = \begin{bmatrix} \frac{1}{\sqrt{3}} & \frac{1}{\sqrt{3}} & \frac{1}{\sqrt{3}} \\ \sqrt{\frac{2}{3}}.cos\theta & \sqrt{\frac{2}{3}}.\cos\left(\theta - \frac{2\pi}{3}\right) & \sqrt{\frac{2}{3}}.\cos\left(\theta + \frac{2\pi}{3}\right) \\ \sqrt{\frac{2}{3}}.sin\theta & \sqrt{\frac{2}{3}}.\sin\left(\theta - \frac{2\pi}{3}\right) & \sqrt{\frac{2}{3}}.\sin\left(\theta + \frac{2\pi}{3}\right) \end{bmatrix} \qquad 0.7$$

Applying this transformation to the 3 phase currents will lead to terms such as $\cos\theta.\sin\omega_2 t$ and this θ can be defined in terms of the base frequency of the machines as given in the equation 2.8.

$$\theta = \omega_1 t + \delta + \pi/2 \qquad 0.8$$

Therefore $\cos\theta.\sin\omega_2 t$ term can be written as in the equation 2.9.

$$cos\theta.sin\omega_2 t = \frac{1}{2}[\sin(\theta + \omega_2 t) - \sin(\theta - \omega_2 t)] \qquad 0.9$$

$$= \frac{1}{2}\{\cos[(\omega_1 + \omega_2)t + \delta] - \cos[(\omega_1 - \omega_2)t + \delta]\}$$

From the equation 2.9, it is clear that currents with frequency $\omega_2$ can be transformed into the currents which contain the frequencies of both the difference and sum of the two frequencies. The differences of two frequencies, $(\omega_1 - \omega_2)$ are termed as sub-synchronous frequencies. Currents with the sub-synchronous frequencies inject energy to the shaft's rotating mass and shaft torques can be produced on the rotor of the turbine-generator. These torques lead to rotor oscillations with the frequencies in the range of sub-synchronous.

The shaft of turbine-generator has natural mechanical oscillation modes typically at the frequency range of sub-synchronous. If the sub-synchronous frequencies of the rotor oscillations caused by shaft torques overlap with the natural mechanical oscillation modes of the rotor shaft, the shaft will start to oscillate at the natural frequency. This is termed as sub-synchronous resonance and this SSR can be led to,

- Stress in shaft and fatigues
- Possible damages
- Failures

## 2.2. Types of Sub-Synchronous Oscillations in Series Capacitor Compensated lines

### 2.2.1. Induction generator effect

This type of oscillations causes by purely electrical phenomenon. Sub-synchronous currents are induced in the armature of the electrical machines by exciting the network resonance frequencies. When consider a constant speed, the rotor of the synchronous machine is rotating at the synchronous speed. This machine speed is faster than the rotating magnetic field's speed which is induced by the armature current in sub-synchronous range. With these conditions the synchronous machine can be considered as performing like an induction machine with a negative slip. When observed from the rotor terminals, the armature resistance is negative with the negative slip. The electrical system is self-excited,

if this negative network resistance exceeds the total network resistance. The self-excitation of the electrical machines will make the current and voltage oscillations grow in the network and eventually can leads to excessive currents and voltages which can damage the generator. [16]

### 2.2.2. Torsional interaction

Torsional interaction is the result of SSR which is coupling between electrical and mechanical phenomenon. In thermal generation units, number of steam turbines are connected to the generator using a long shaft. The mechanical system of a thermal generation unit has a number of natural frequencies, because of this multi mass unit. Disturbances in both mechanical and electrical systems energize the natural modes. Therefore, the mechanical torque in the turbine shaft system consists of its natural frequencies and the electromagnetic torque developed by the currents in armature contain with sub-synchronous frequency components corresponding to the network resonances. If the induced sub-synchronous frequency in the electromechanical torque is close enough to a natural frequency of the shaft of turbine-generator system, the oscillations of the electrical system can aid to increase the oscillations in the mechanical system and vice versa. This phenomenon is known as the torsional interaction. [16]

### 2.2.3. Transient torques

Transient torques are also resulting from SSR which is coupling between electrical and mechanical phenomenon. Result from the disturbances in the system can be lead to unexpected variations in the network, and thus the variations in currents can cause to oscillate at the network natural frequencies. If any of those sub-synchronous network frequencies overlap with a natural mode of a shaft of turbine-generator, large peak torques which are proportional to the oscillating currents' magnitude can be produced. Currents produced by short circuits may develop very large torques on shaft when there is a fault applied and cleared. [16]

## 2.3.Proposed Techniques to mitigate sub-synchronous oscillations

Both synchronous and induction machines are self-excited by installing capacitors in series on power transmission lines and it has been known for many years. But the harshness of the harmful effects of series capacitors apply on electrical machines get attention only after the failure of one of the exciter shafts in a machine at the Mohave power station in October 1971 [6]. From this point several researches have been achieved to investigate the SSR of synchronous generators with series capacitor compensated power transmission lines and other devices such as HVDC converter terminals.

### 2.3.1. Conventional solutions to problems with SSR

The following solutions were proposed as conventional solutions to mitigate the effects of SSR on generating units and power systems.

- Static filter

For recognized SSR modes in a system, a static filter can be used with a particular bandwidth. A static filter arrangement can be either a damping circuit or a L-C filter. To avoid sub-synchronous currents flowing again to the generator, the filter has to be in series when located at the generator side. Otherwise, the static filter and the fixed series compensation can be connected in parallel by way of a damping circuit.

- Dynamic filter

For several SSR modes, the dynamic filter is self-adaptable. Typically, connect a dynamic filter with the generator unit in series and the derivation of the speed of the rotor has been picked as the input for the frequency extraction of the SSR occurrence. When a sub-synchronous component is sensed, a reverse direction sub-synchronous voltage can be produced by the dynamic filter. The produced voltage can compensate the armature voltage in sub-synchronous range.

- Dynamic stabilizer

Dynamic stabilizer is consisted with shunt reactors which are controlled by thyristors. These reactors are linked with the generator to control sub-synchronous oscillations. Normally, a reactor connected in parallel is located at the generator low voltage winding for the reactive power absorbing. The shunt reactors can be applied for SSR mitigation by regulating thyristor units. The input is the speed derivation of the generator rotor and the suitable waveforms can be produced by regulating thyristor units. The waveforms produced by the thyristor units can be used to mitigate the sub-synchronous oscillation by circulate them in the parallel circuit.

- Protective relays

Among the countermeasures of SSR, use of protective relays is a common method. A protective relay is able to sense SSR happening in a network and the control signals can be send to activate other units like circuit breakers or by-pass switches. The SSR occurrence can be detected by either identifying speed of the rotor or identifying the current flow of the generator armature.

By help of the installation of protective relays and filters, SSR mitigation is mainly achieved in previously. However, some potential solutions are also existed with power electronic based FACTS technology which was suggested by the researchers. The proposed SSR mitigating arrangements which are built on the controllability of devices with power electronics such as Static Var Compensator (SVC), Static Synchronous Compensator (STATCOM) and Thyristor Controlled Series Compensation (TCSC) are discussed in the following sections.

### 2.3.2. Solutions from FACTS Devices

FACTS devices were developed rapidly through the past years. A better control for the power system is allowed by these FACTS devices and there are several key parameters such as the impedance of the system or the voltage at terminals.

FACTS devices use a power electronic based technology which leads to a quick response for the system dynamics. From the FACT devices-based solutions the gaps between different levels of control can be reduced and for a smooth operation of the system, consent an advanced controllability. To control the parameters of the systems smoothly, several FACTS devices have been proposed. A few widely used FACTS devices to mitigate SSR are listed here.

#### 2.3.2.1. Static VAr Compensator (SVC)

SVC has the capability of delivering and receiving the reactive power by connecting in parallel. SVC can be applied to compensate the reactive power, control the voltage, damp low-frequency oscillations and increase the stability in the power systems. The reference [8] and [9] present two researches did on mitigating of the SSR in power systems by using SVC.

The reference [8], uses the optimal control of SVC to damp the SSR in IEEE FBM model. The linearized system is used to derive the state space representation of the system. Then, the system stability is obtained by shifting the eigenvalues of the test system to the left of the imaginary axis. It's noticed that a respectable damping for the SSR is provided by the optimum control and the system is stable for the power factor and the active power in selected range.

The paper presents from reference [9], validates that grid connected wind farms with a series capacitor compensation in power transmission line can have the sub-synchronous oscillations. The selected power system is modelled using dynamic phasors to obtain the small signal model. An SVC is used to damp the sub-synchronous oscillations while the

line current is selected as the feedback signal. The results were applied and demonstrated to a huge practical power system. When use the SVC in networks, these researches only consider about the mitigation of SSR. But the SVC is developed not only to control the SSR and it can affect for system in another away. These researches are focus only for a unique operating point of the system.

#### 2.3.2.2. Static Synchronous Series Compensator (SSSC)

SSSC is a series connected device which consists with a voltage source inverter and through a coupling transformer, it connect to the transmission line. By adjusting the phase angles of voltage and current, SSSC assists for a smooth control through the system impedance. Hence, SSSC supports for the stability control of the system and power flow control as well. The reference [10] and [11] present two researches which use the SSSC to mitigate of the SSR in power systems.

In both reference [10] and [11], IEEE first benchmark model is selected to analysis the designed controller and reference [10] selects the compensation level of the transmission line as 55%. The paper presents from reference [10], proposes a fuzzy logic control (FLC) for SSSC to damp the oscillations caused by SSR. SSSC base on FLC, provided better results in rotor angle deviations, speed deviation and torque deviation by increasing its damping and decreasing its steady state error. The paper presents from reference [11], use SSSC to damp the sub-synchronous resonance with hysteresis current control. The validity of the proposed controller by using SSSC, to reduce SSR due to the torsional interaction is shown in [11].

#### 2.3.2.3. Static Synchronous Compensator (STATCOM)

STATCOM is another FACT device comparable to SVC but it gives a quicker response to the variations in voltage when use for controlling of the reactive power. The practice of STATCOM to mitigate SSR is shown from two research papers, reference [12] and [13]. Both researches select IEEE first benchmark model as the test system. Reference [12]

selects 60% of series compensation level of the transmission line and reference [13] selects 18% to 33% of compensation level of the transmission line.

In reference [12], active compensation connected in parallel and passive compensation connected in series presents by a STATCOM coupled at the electrical center of the power transmission line are studied. An auxiliary sub-synchronous damping controller (SSDC) with STATCOM used to damp the SSR produced by series capacitors. From the results of this research, it shows that the SSR network characteristics are not changed significantly due to the presence of STATCOM and properly designed SSDC is required to damp critical torsional modes. In reference [13], integrating combined a wind turbine based on self-excited induction generator is used to achieve the goal. It's examined that the potential occurrence and mitigation of the SSR in a series compensated wind park, produced by the effects of induction generator and the torsional interactions. In the simulation results of this research the controllers for mitigate SSR because of the raise of the series capacitor compensation of the wind power plant compensated in series, perform well (compensation level is increased only up to 33%). When designing the control loops for damping to the STATCOM, the damping torque analysis is used. Therefore, for the torsional mode frequencies, a net positive damping torque is provided. The proposed damping control system decreases the highest point of the negative torque and protected greater margin of stability which is called as the values of maximum time taken for fault clearing and the critical speed of the induction generator rotors in the wind plant. The results from the simulations of this research present a new method of using STATCOM for huge series capacitor compensated wind power plants which expands the transient stability margin significantly.

#### 2.3.2.4. Thyristor-Controlled Series Compensator (TCSC)

TCSC is targeting to providing a smooth control through the system impedance by connecting it in series with the system. TCSC consist with a series capacitor paralleled by a reactor which is controlled by thyristors. Mainly TCSC is applied for the controlling and

enhancing of power flow, stability improving and SSR mitigating. Two researches done on SSR mitigation of IEEE first benchmark model with the help of TCSC are given in reference [14] and [15]. The SSR torques of the electromechanical system was analysis and damped in these researches. In reference [15], the eigenvalue methods and MATLAB Simulink has been implemented for the analysis. It shows that, at the specified operating point, the basic electromechanical system is unstable without TCSC. The TCSC is coupled at the receiving end of the power transmission line control by the TCSC controller. Also, it shows that, the critical torsional mode (with 56% of compensation level) is stabilized with decent stability margin, when the TCSC is controlled with PI controller.

## 2.4.Defects of the existing systems

Presently, there are many solutions invent to damp the sub-synchronous oscillations and many researches prove that controlling methods are valid for specify operating points on the system. The latest control technologies consist with power electronic based FACT devices such as SVC, TCSC and STATCOM. These FACT devices are designed not only to damp sub-synchronous resonance but also for many other options such as reactive power control. Therefore, although these FACT controllers damped the sub-synchronous oscillations, they may adversely affect on other oscillatory modes. These FACT devices have operating limitations and therefore the controllers may not perform well under several operating points of the system. The researches also validate these controllers only with one or two operating points of the system. Hence, a robust PID controller which can perform well under different operating conditions was designed as describe in following sections

## 2.5.Objectives of the research

The main goal of this research is to design a robust controller to damp dominant sub-synchronous oscillations and compare its performance with other existing types of controllers. The implemented controller performs well in a specific range of operating points of the system. The following approaches are proposed in this thesis to achieve the above objectives.

1. Develop a linearized state space representation of an IEEE benchmark system and investigate the sub-synchronous oscillations.
2. Design a robust controller to damp out dominant sub-synchronous oscillations.
3. Assess the performance of the designed robust controller with different operating points in the system.

As describe in this chapter, different techniques are used to mitigate the sub-synchronous oscillations and nowadays power electronic based FACTs devices are mostly used for this purpose. These devices are designed for other power system operations such as reactive power control but not for mitigate sub-synchronous oscillation. However, these devices are used for SSO mitigating by adding different changes. Therefore, these controlling methods contain several defects as discussed. Objective of this research is to design a robust controller which can perform better than the existing controllers in different operating points of the selected test system to mitigate the sub-synchronous oscillations.

# CHAPTER 03

# METHODOLOGY

## 3.1. Develop a linearized state space representation of the selected test system

Unstable or undamped electromechanical oscillations that are natural for the interconnected systems are one of the main reasons of large-scale power system blackouts. Because of several aspects such as dynamic complexity, increase of size and power system utilization arrangement of suitable damping inhabits a significant research challenge. There is a set of models of power system for benchmark as suggested by the IEEE Task Force on Benchmark Systems for Stability Controls which was initiated by the Power System Stability Controls Subcommittee of the Power System Dynamic Performance Committee [20]. The 'Benchmark system' is a power system model which contains a set of conventional stabilizers in the power system and these power system benchmark models give a reference for measuring the performance of the damping of several damping controllers and regulation methods for the research community.

First, one of these benchmark models should be selected as the test system. The non-linear models of these IEEE benchmark models can find from the examples of PSCAD software and have to derive the linearized model for further works. To study SSR events, there are several study tools such as scanning of frequency, complex torque coefficient and analysis of eigenvalues.

Among these methods, analysis of eigenvalue method was used for study the SSR event. Sub-synchronous oscillations and resonance can be observed from the frequencies of the eigenvalues obtain from the linearized test system. The linearized state space representation of the selected power system should be in the form of equation 3.1 and 3.2.

Eigenvalues of the power system can be observed from the state matrix ($A$) of equation 3.1.

$$\Delta\dot{X} = A\Delta X + B\Delta U \quad 3.1$$

$$\Delta Y = C\Delta X \quad 3.2$$

### 3.2. Validate the linearized model

The test system has to be linearized by ignoring the higher order terms using Taylor series. Hence, final linearized model should check for the validation with the non-linearized model. Frequencies of the power system were considered for this validation. If the frequencies of the output waveform of the linearized model are matched with output waveform frequencies of the nonlinear model, linearized model can be assumed to be correctly representing the linear dynamics at the operating point. The FFT analysis tool in MATLAB can be used for this frequency analyze.

### 3.3. Designing the controller

A robust controller should design to damp out the sub-synchronous oscillations of the selected test system. A PID controller is proposed with a suitable method of optimization to perform well under different operating conditions. The operating point of the test system is changed by varying the compensation percentage. Series capacitor compensation level is the percentage of the capacitor value connected series in the transmission line with the total inductor value of the transmission line. Hence, the operating point of the test system can be changed by changing the series connected capacitor value in the transmission line.

Then, the designed controller's performance should be evaluated with several operating points by using the linearized system and the original nonlinear test system.

# CHAPTER 04

# MODELLING THE SYSTEM

## 4.1. Test system

IEEE FBM was selected for this study as the test system. IEEE Working Group on Sub-Synchronous Resonance developed the IEEE FBM in 1977 to implement a model for the benchmark which can be applied as a reference for the evaluation of several approaches of computer-related simulations and analysis [20]. As shown in Figure 4.1, the system comprises a single generator and a series capacitor compensated transmission line is used to connect the generator to an infinite bus. The following section explain the procedure for deriving the linearized model of IEEE FBM model.

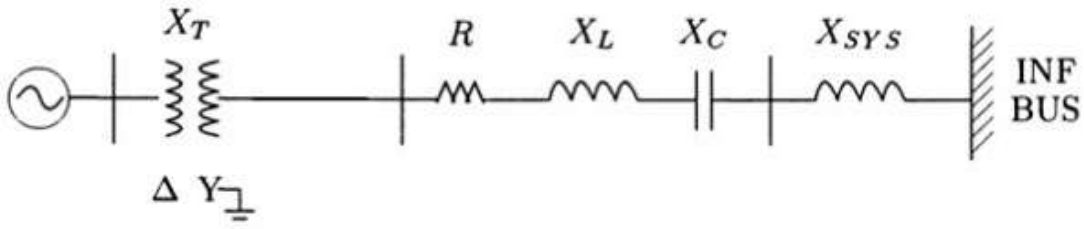


*Figure 4.1: IEEE first benchmark model*

The Table 4.1 shows the per unit values of the network impedances on the base of 892.4 MVA [18].

*Table 4.1: Per unit values of the network impedance on the base of 892.4 MVA*

| Parameter | Positive Sequence of the impedance | Zero Sequence of the impedance |
|---|---|---|
| R | 0.02 | 0.5 |
| $X_T$ | 0.14 | 0.14 |

| | | |
|---|---|---|
| $X_L$ | 0.5 | 1.56 |
| $X_{sys}$ | 0.06 | 0.06 |
| $X_C$ (70% compensation) | 0.35 | 0.35 |

The rotor model of the IEEE FBM is given from the Figure 4.2. This is represented with several turbine units which can modelled separately. Table 4.2 gives the data of the rotor model.

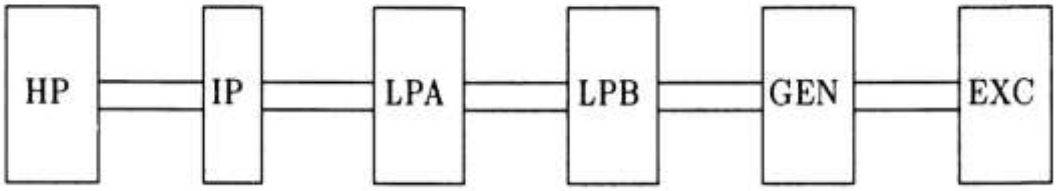


*Figure 4.2: rotor model of the IEEE FBM*

*Table 4.2: Data of the IEEE FBM rotor model*

| | Inertia constant, H | Shaft section | Spring Constant, K in p.u. T/rad |
|---|---|---|---|
| High Pressure turbine (HP) | 0.0929 | HP-IP | 19.303 |
| Intermediate Pressure turbine (IP) | 0.1556 | IP-LPA | 34.929 |
| Low Pressure A turbine (LPA) | 0.8587 | LPA-LPB | 52.038 |
| Low Pressure B turbine (LPB) | 0.8842 | LPB-GEN | 70.858 |
| Generator (GEN) | 0.8685 | GEN-EXC | 2.82 |
| Exciter (EXC) | 0.0342 | | |

The non-linear model of IEEE FBM is already modelled in PSCAD software. Figure 4.3 illustrates the PSCAD model of FBM with 70% of series capacitor compensation and the transmission line is subjected to a three-phase ground fault at 1.5 seconds. In this PSCAD model the synchronous generator take 1.1 seconds to enable. Simulation results of some variable such as speed of the generator, load angle, generator output voltage, with and without the series compensation are shown in figure 4.4 and 4.5 respectively.

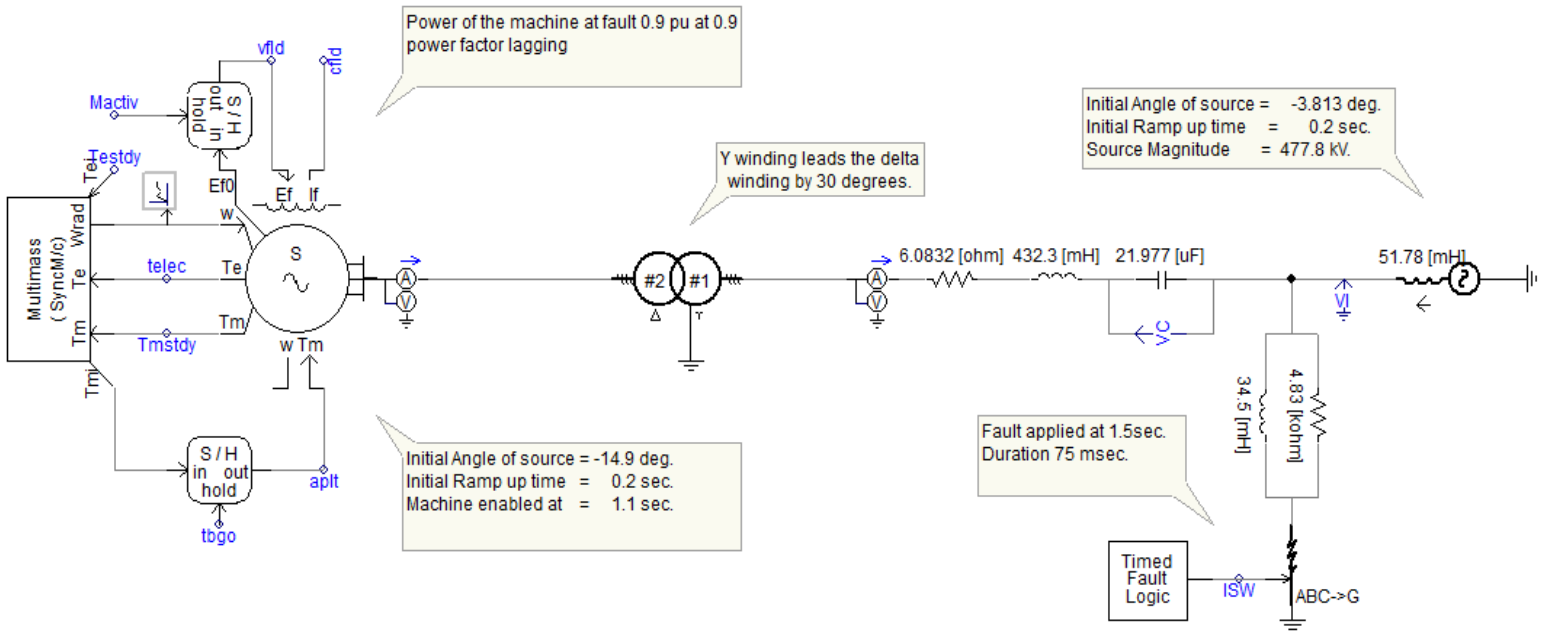


*Figure 4.3: PSCAD model of IEEE FBM with 70% series compensation level and a three-phase to ground fault at 1.5 s.*

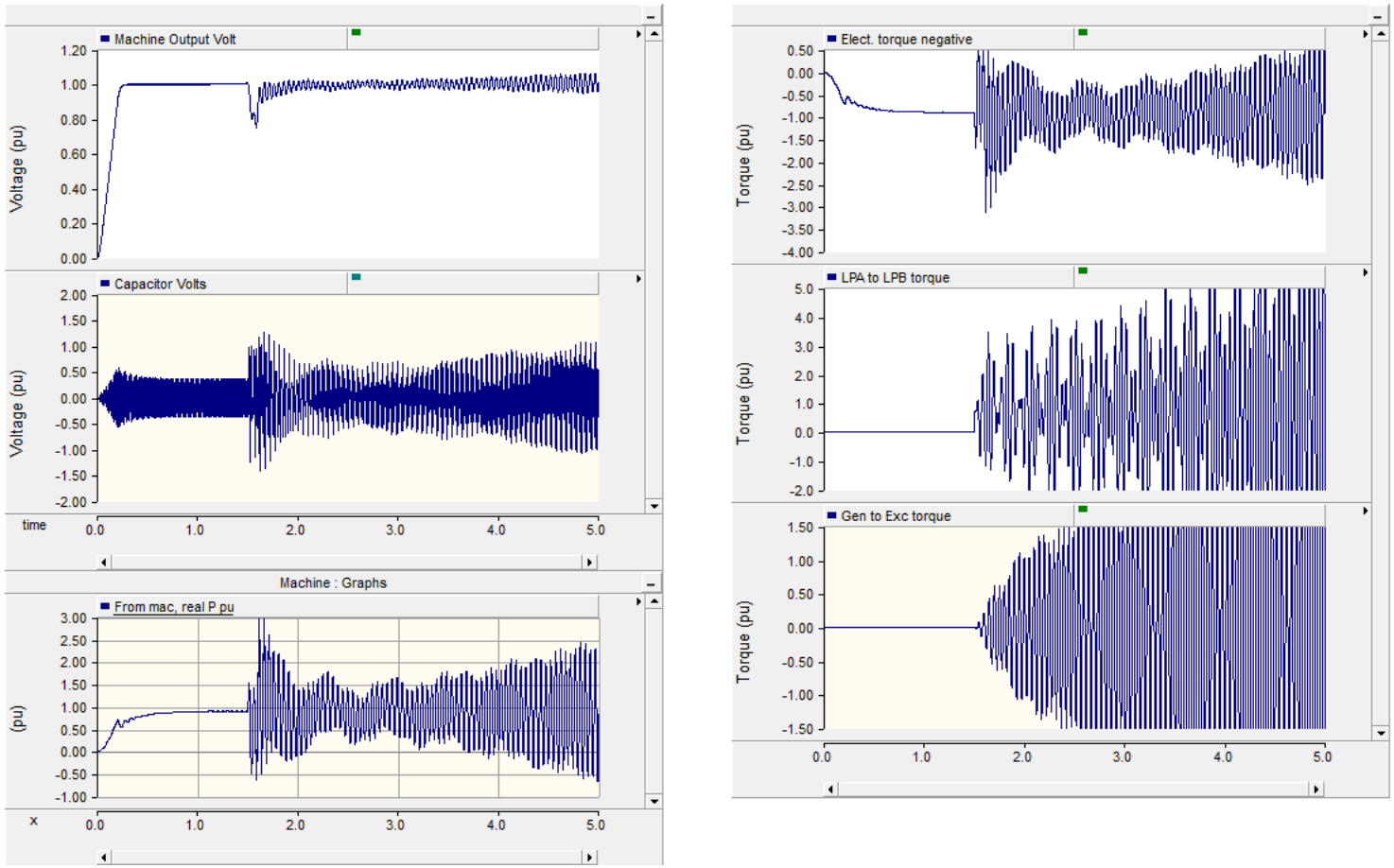


*Figure 4.4: Simulation results of IEEE FBM with series compensation*

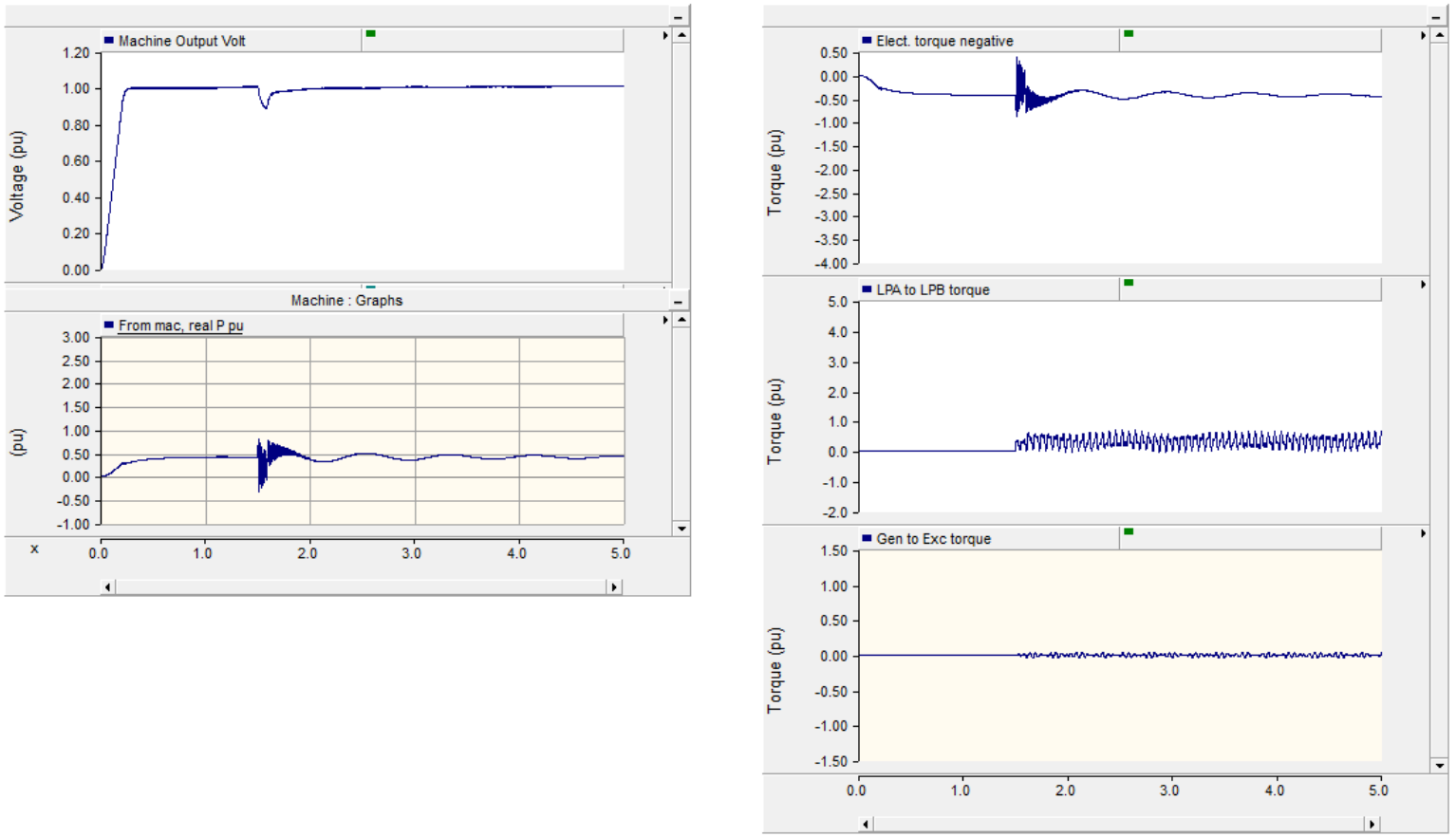


*Figure 4.5: Simulation results of IEEE FBM without series compensation*

### 4.1.1. Conventional generator model

Without considering the stator transients the synchronous generator was modeled using $6^{th}$ order model. This generator model represents the dynamic behavior of the generator rotor, field winding along the d-axis and two damper windings along q-axis. Equations from 4.1 to 4.6 show the corresponding differential equations and figure 4.6 illustrates the equivalent circuit of the synchronous generator. And the synchronous generator machine parameters with 892.4 MVA base is given in table 4.2.

*Table 4.3: Synchronous generator machine parameters with 892.4 MVA base*

| Parameter | Units(p.u.) | Parameter | Units(p.u.) | Parameter | Units(p.u.) |
|---|---|---|---|---|---|
| $L_d$ | 1.79 | $T_{d0p}$ | 4.3 | $L_{ad}$, $L_{aq}$ | 1.666, 1.58 |
| $L_q$ | 1.71 | $T_{q0p}$ | 0.032 | $R_{fd}$, $L_{fd}$ | 0.011, 1.7 |
| $R_a$ | 0.0015 | $T_{d0pp}$ | 0.85 | $R_{1d}$ | 0.0037 |
| $L_{dp}$ | 0.169 | $T_{q0pp}$ | 0.05 | $L_{1d}$ | 1.666 |
| $L_{dpp}$ | 0.228 | $T_{dp}$ | 0.40598 | $R_{1q}$ | 0.0053 |
| $L_q$ | 0.135 | $T_{qp}$ | 0.02556 | $L_{1q}$ | 0.695 |
| $L_{qp}$ | 0.2 | $T_{dpp}$ | 0.11333 | $R_{2q}$ | 0.0182 |
| $L_{qpp}$ | 0.13 | $T_{qpp}$ | 0.04386 | $R_{2q}$ | 1.825 |

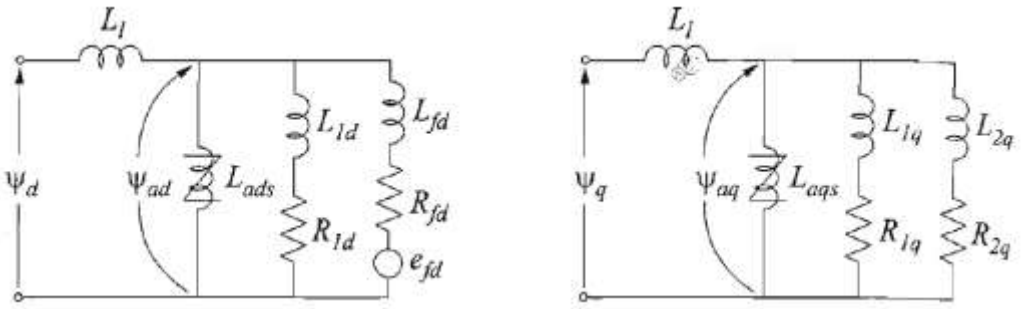


*Figure 4.6: Equivalent circuit of the synchronous generator*

$$\Delta\dot{\omega}_r = \frac{1}{2H}\{T_m - (\varphi_{ad} i_q - \varphi_{aq} i_d) - K_D \Delta\omega_r\} \quad 4.1$$

$$\dot{\delta} = \omega_0 \, \Delta\omega_r \quad 4.2$$

$$\dot{\varphi_{fd}} = \frac{\omega_0 R_{fd}}{L_{ad}} E_{fd} - \frac{\omega_0 R_{fd}}{L_{fd}} \varphi_{fd} + \frac{\omega_0 R_{fd}}{L_{fd}} \left[ L_{adpp} \left( -i_d + \frac{\varphi_{fd}}{L_{fd}} + \frac{\varphi_{1d}}{L_{1d}} \right) \right] \quad 4.3$$

$$\dot{\varphi_{1d}} = \frac{-\omega_0 R_{1d}}{L_{1d}} \varphi_{1d} + \frac{\omega_0 R_{1d}}{L_{1d}} \left[ L_{adpp} \left( -i_d + \frac{\varphi_{fd}}{L_{fd}} + \frac{\varphi_{1d}}{L_{1d}} \right) \right] \quad 4.4$$

$$\dot{\varphi_{1q}} = \frac{-\omega_0 R_{1q}}{L_{1q}} \varphi_{1q} + \frac{\omega_0 R_{1q}}{L_{1q}} \left[ L_{aqpp} \left( -i_q + \frac{\varphi_{1q}}{L_{1q}} + \frac{\varphi_{2q}}{L_{2q}} \right) \right] \quad 4.5$$

$$\dot{\varphi_{2q}} = \frac{-\omega_0 R_{2q}}{L_{2q}} \varphi_{2q} + \frac{\omega_0 R_{2q}}{L_{2q}} \left[ L_{aqpp} \left( -i_q + \frac{\varphi_{1q}}{L_{1q}} + \frac{\varphi_{2q}}{L_{2q}} \right) \right] \quad 4.6$$

Where,

$$\varphi_{ad} = L_{adpp} \left( -i_d + \frac{\varphi_{fd}}{L_{fd}} + \frac{\varphi_{1d}}{L_{1d}} \right)$$

$$\varphi_{aq} = L_{aqpp} \left( -i_q + \frac{\varphi_{1q}}{L_{1q}} + \frac{\varphi_{2q}}{L_{2q}} \right)$$

$$L_{adpp} = \frac{1}{\frac{1}{L_{ad}} + \frac{1}{L_{fd}} + \frac{1}{L_{1d}}}$$

$$L_{aqpp} = \frac{1}{\frac{1}{L_{aq}} + \frac{1}{L_{1q}} + \frac{1}{L_{2q}}}$$

By using Taylor series, equations for small signal model were derive and given by the equations from 4.7 to 4.12.

$$\begin{aligned}\Delta\dot{\omega}_r = &-\frac{K_D}{2H}\Delta\omega_r - \frac{L_{adpp} i_{q0}}{2HL_{fd}}\Delta\varphi_{fd} - \frac{L_{adpp} i_{q0}}{2HL_{1d}}\Delta\varphi_{1d} + \frac{L_{aqpp} i_{d0}}{2HL_{1q}}\Delta\varphi_{1q} \\ &+ \frac{L_{aqpp} i_{d0}}{2HL_{2q}}\Delta\varphi_{2q} + \left(-\frac{\varphi_{ad}}{2H} - \frac{L_{aqpp} i_{d0}}{2H}\right)\Delta i_q \\ &+ \left(\frac{\varphi_{aq}}{2H} + \frac{L_{adpp} i_{q0}}{2H}\right)\Delta i_d + \frac{1}{2H}\Delta T_m\end{aligned} \qquad 4.7$$

$$\Delta\dot{\delta} = \omega_0\,\Delta\omega_r \qquad 4.8$$

$$\begin{aligned}\Delta\dot{\varphi}_{fd} = &\left(-\frac{\omega_0 R_{fd}}{L_{fd}} + \frac{\omega_0 R_{fd} L_{adpp}}{L_{fd}^2}\right)\Delta\varphi_{fd} + \frac{\omega_0 R_{fd} L_{adpp}}{L_{fd} L_{1d}}\Delta\varphi_{1d} \\ &- \frac{\omega_0 R_{fd} L_{adpp}}{L_{fd}}\Delta i_d + \frac{\omega_0 R_{fd}}{L_{ad}}\Delta E_{fd}\end{aligned} \qquad 4.9$$

$$\begin{aligned}\Delta\dot{\varphi}_{1d} = &\left(-\frac{\omega_0 R_{1d}}{L_{1d}} + \frac{\omega_0 R_{1d} L_{adpp}}{L_{1d}^2}\right)\Delta\varphi_{1d} + \frac{\omega_0 R_{1d} L_{adpp}}{L_{1d} L_{fd}}\Delta\varphi_{fd} \\ &- \frac{\omega_0 R_{1d} L_{adpp}}{L_{1d}}\Delta i_d\end{aligned} \qquad 4.10$$

$$\Delta\dot{\varphi}_{1q} = \left(-\frac{\omega_0 R_{1q}}{L_{1q}} + \frac{\omega_0 R_{1q} L_{aqpp}}{L_{1q}^2}\right)\Delta\varphi_{1q} + \frac{\omega_0 R_{1q} L_{aqpp}}{L_{1q} L_{2q}}\Delta\varphi_{2q} - \frac{\omega_0 R_{1q} L_{aqpp}}{L_{1q}}\Delta i_q \quad 4.11$$

$$\Delta\dot{\varphi}_{2q} = \left(-\frac{\omega_0 R_{2q}}{L_{2q}} + \frac{\omega_0 R_{2q} L_{aqpp}}{L_{2q}^2}\right)\Delta\varphi_{2q} + \frac{\omega_0 R_{2q} L_{aqpp}}{L_{2q} L_{1q}}\Delta\varphi_{1q} - \frac{\omega_0 R_{2q} L_{aqpp}}{L_{2q}}\Delta i_q \quad 4.12$$

The generator state space model is given by equation 4.13. The model is given in the form of $\Delta\dot{X}_{ga} = A_{ga}\Delta X_{ga} + B_{ga}\Delta U_{ga} + C_{ga}\Delta I_{ga}$. There are six state variables, rotor speed ($\omega_r$), rotor angle ($\delta$), d-axis field winding flux ($\varphi_{fd}$), d-axis damper winding flux ($\varphi_{1d}$), q-axis first damper winding flux ($\varphi_{1q}$) and q-axis second damper winding flux ($\varphi_{2q}$) and two inputs: mechanical torque ($T_m$) and voltage applied to the field winding ($E_{fd}$) in the system.

$$\begin{bmatrix} \Delta\dot{\omega}_r \\ \Delta\dot{\delta} \\ \Delta\dot{\varphi}_{fd} \\ \Delta\dot{\varphi}_{1d} \\ \Delta\dot{\varphi}_{1q} \\ \Delta\dot{\varphi}_{2q} \end{bmatrix} = \begin{bmatrix} a_{11a} & 0 & a_{13a} & a_{14a} & a_{15a} & a_{16a} \\ a_{21a} & 0 & 0 & 0 & 0 & 0 \\ 0 & 0 & a_{33a} & a_{34a} & 0 & 0 \\ 0 & 0 & a_{43a} & a_{44a} & 0 & 0 \\ 0 & 0 & 0 & 0 & a_{55a} & a_{56a} \\ 0 & 0 & 0 & 0 & a_{65a} & a_{66a} \end{bmatrix} \begin{bmatrix} \Delta\omega_r \\ \Delta\delta \\ \Delta\varphi_{fd} \\ \Delta\varphi_{1d} \\ \Delta\varphi_{1q} \\ \Delta\varphi_{2q} \end{bmatrix} + \begin{bmatrix} b_{11a} & 0 \\ 0 & 0 \\ 0 & b_{32a} \\ 0 & 0 \\ 0 & 0 \\ 0 & 0 \end{bmatrix} \begin{bmatrix} \Delta T_m \\ \Delta E_{fd} \end{bmatrix} + \begin{bmatrix} i_{11a} & i_{12a} \\ 0 & 0 \\ i_{31a} & 0 \\ i_{41a} & 0 \\ 0 & i_{52a} \\ 0 & i_{62a} \end{bmatrix} \begin{bmatrix} \Delta i_d \\ \Delta i_q \end{bmatrix} \quad 4.13$$

The parameters of the $A_{ga}$ matrix are given by,

$$a_{11a} = -\frac{K_D}{2H}$$

$$a_{13a} = -\frac{L_{adpp} i_{q0}}{2HL_{fd}}$$

$$a_{14a} = -\frac{L_{adpp} i_{q0}}{2HL_{1d}}$$

$$a_{15a} = \frac{L_{aqpp} i_{d0}}{2HL_{1q}}$$

$$a_{16a} = \frac{L_{aqpp} i_{d0}}{2HL_{2q}}$$

$$a_{21a} = \omega_0$$

$$a_{33a} = \left(-\frac{\omega_0 R_{fd}}{L_{fd}} + \frac{\omega_0 R_{fd} L_{adpp}}{L_{fd}^2}\right)$$

$$a_{34a} = \frac{\omega_0 R_{fd} L_{adpp}}{L_{fd} L_{1d}}$$

$$a_{43a} = \frac{\omega_0 R_{1d} L_{adpp}}{L_{1d} L_{fd}}$$

$$a_{44a} = \left(-\frac{\omega_0 R_{1d}}{L_{1d}} + \frac{\omega_0 R_{1d} L_{adpp}}{L_{1d}^2}\right)$$

$$a_{55a} = \left(-\frac{\omega_0 R_{1q}}{L_{1q}} + \frac{\omega_0 R_{1q} L_{aqpp}}{L_{1q}^2}\right)$$

$$a_{56a} = \frac{\omega_0 R_{1q} L_{aqpp}}{L_{1q} L_{2q}}$$

$$a_{65a} = \frac{\omega_0 R_{2q} L_{aqpp}}{L_{2q} L_{1q}}$$

$$a_{66a} = \left(-\frac{\omega_0 R_{2q}}{L_{2q}} + \frac{\omega_0 R_{2q} L_{aqpp}}{L_{2q}^2}\right)$$

The parameters of the $B_{ga}$ matrix are given by,

$$b_{11a} = \frac{1}{2H}$$

$$b_{32a} = \frac{\omega_0 R_{fd}}{L_{ad}}$$

The parameters of the $C_{ga}$ matrix are given by,

$$i_{11a} = \left(\frac{\varphi_{aq}}{2H} + \frac{L_{adpp} i_{q0}}{2H}\right)$$

$$i_{12a} = \left(-\frac{\varphi_{ad}}{2H} - \frac{L_{aqpp} i_{d0}}{2H}\right)$$

$$i_{31a} = -\frac{\omega_0 R_{fd} L_{adpp}}{L_{fd}}$$

$$i_{41a} = -\frac{\omega_0 R_{1d} L_{adpp}}{L_{1d}}$$

$$i_{52a} = -\frac{\omega_0 R_{1q} L_{aqpp}}{L_{1q}}$$

$$i_{62a} = -\frac{\omega_0 R_{2q} L_{aqpp}}{L_{2q}}$$

### 4.1.2. Generator model including stator transients

To observe the sub-synchronous oscillations, AC network was represented using a dynamic phasor model in this study. In that case two additional differential equations were used to represent the stator dynamics in d and q axes. Therefore, an 8th order model for the round rotor type generator was formulated.

When consider the stator transient, currents in d and q axes can be represented by the equations 4.14 and 4.15 respectively.

$$\Delta i_d = K_{d3b}\Delta\varphi_d + K_{d4b}\Delta\varphi_{fd} + K_{d5b}\Delta\varphi_{1d} \qquad 4.14$$

$$\Delta i_q = K_{q6b}\Delta\varphi_q + K_{q7b}\Delta\varphi_{1q} + K_{q8b}\Delta\varphi_{2q} \qquad 4.15$$

Where,

$$K_{d3b} = -\frac{L_{ad}L_{dpp}(L_{fd}+L_{1d})}{L_l L_d L_{fd} L_{1d}} - \frac{1}{L_d}$$

$$K_{d4b} = \frac{L_{dpp}}{L_l L_{fd}}$$

$$K_{d5b} = \frac{L_{dpp}}{L_l L_{1d}}$$

$$L_{dpp} = \frac{1}{\frac{1}{L_l}+\frac{1}{L_{ad}}+\frac{1}{L_{fd}}+\frac{1}{L_{1d}}}$$

$$K_{q6b} = -\frac{L_{aq}L_{qpp}(L_{1q}+L_{2q})}{L_l L_q L_{1q} L_{2q}} - \frac{1}{L_q}$$

$$K_{q7b} = \frac{L_{qpp}}{L_l L_{1q}}$$

$$K_{q8b} = \frac{L_{qpp}}{L_l L_{2q}}$$

$$L_{qpp} = \frac{1}{\frac{1}{L_l}+\frac{1}{L_{aq}}+\frac{1}{L_{1q}}+\frac{1}{L_{2q}}}$$

Equations for stator transient are given in equations 4.16 and 4.17.

$$\dot{\varphi_d} = [e_d + \omega_r \varphi_q + R_a i_d]\omega_0 \qquad 4.16$$

$$\dot{\varphi_q} = [e_q + \omega_r \varphi_d + R_a i_q]\omega_0 \qquad 4.17$$

Equations 4.18 and 4.19 represent the linearized equations, of these non-linear equations (equation 4.16 and 4.17) which were linearized by using Taylor Series.

$$\Delta\dot{\varphi}_d = [\Delta e_d + \omega_r \Delta\varphi_q + R_a \Delta i_d]\omega_0 \qquad 4.18$$

$$\Delta\dot{\varphi}_q = [\Delta e_q + \omega_r \Delta\varphi_d + R_a \Delta i_q]\omega_0 \qquad 4.19$$

$\Delta i_d$ and $\Delta i_q$ of equations 4.18,4.19 and 4.13 can be replaced by using equations 4.14 and 4.15.

Then the 8th order generator state space model is given by equation 4.20. The model is given in the form of $\Delta\dot{X}_{gb} = A_{gb}\Delta X_{gb} + B_{gb}\Delta U_{gb} + D_{gb}\Delta E_{gb}$. There are 8 state variables, rotor speed ($\omega_r$), rotor angle ($\delta$), flux of the d-axis stator winding ($\varphi_d$), flux of the d-axis field winding ($\varphi_{fd}$), flux of the damper winding of d-axis ($\varphi_{1d}$), flux of the q-axis stator winding ($\varphi_q$), flux of the q-axis first damper winding ($\varphi_{1q}$) and flux of the q-axis second damper winding ($\varphi_{2q}$) and two inputs: mechanical torque ($T_m$) and voltage applied to the field winding ($E_{fd}$) in the system.

$$\begin{bmatrix} \Delta\dot{\omega}_r \\ \Delta\dot{\delta} \\ \Delta\dot{\varphi}_d \\ \Delta\dot{\varphi}_{fd} \\ \Delta\dot{\varphi}_{1d} \\ \Delta\dot{\varphi}_q \\ \Delta\dot{\varphi}_{1q} \\ \Delta\dot{\varphi}_{2q} \end{bmatrix} = \begin{bmatrix} a_{11b} & 0 & a_{13b} & a_{14b} & a_{15b} & a_{16b} & a_{17b} & a_{18b} \\ a_{21b} & 0 & 0 & 0 & 0 & 0 & 0 & 0 \\ 0 & 0 & a_{33b} & a_{34b} & a_{35b} & a_{36b} & 0 & 0 \\ 0 & 0 & a_{43b} & a_{44b} & a_{45b} & 0 & 0 & 0 \\ 0 & 0 & a_{53b} & a_{54b} & a_{55b} & 0 & 0 & 0 \\ 0 & 0 & a_{63b} & 0 & 0 & a_{66b} & a_{67b} & a_{68b} \\ 0 & 0 & 0 & 0 & 0 & a_{76b} & a_{77b} & a_{78b} \\ 0 & 0 & 0 & 0 & 0 & a_{86b} & a_{87b} & a_{88b} \end{bmatrix} \begin{bmatrix} \Delta\omega_r \\ \Delta\delta \\ \Delta\varphi_d \\ \Delta\varphi_{fd} \\ \Delta\varphi_{1d} \\ \Delta\varphi_q \\ \Delta\varphi_{1q} \\ \Delta\varphi_{2q} \end{bmatrix} \quad 4.20$$

$$+ \begin{bmatrix} b_{11b} & 0 \\ 0 & 0 \\ 0 & 0 \\ 0 & b_{42b} \\ 0 & 0 \\ 0 & 0 \\ 0 & 0 \\ 0 & 0 \end{bmatrix} \begin{bmatrix} \Delta T_m \\ \Delta E_{fd} \end{bmatrix} + \begin{bmatrix} 0 & 0 \\ 0 & 0 \\ d_{31b} & 0 \\ 0 & 0 \\ 0 & 0 \\ 0 & d_{62b} \\ 0 & 0 \\ 0 & 0 \end{bmatrix} \begin{bmatrix} \Delta e_d \\ \Delta e_q \end{bmatrix}$$

The parameters of the $A_{ga}$ matrix is given by,

$$a_{11b} = -\frac{K_D}{2H} \qquad a_{53b} = -K_{d3b}\frac{\omega_0 R_{1d} L_{adpp}}{L_{1d}}$$

$$a_{13b} = K_{d3b}\left(\frac{\varphi_{aq}}{2H} + \frac{L_{adpp} i_{q0}}{2H}\right) \qquad a_{54b} = \frac{\omega_0 R_{1d} L_{adpp}}{L_{1d} L_{fd}} - K_{d4b}\frac{\omega_0 R_{1d} L_{adpp}}{L_{1d}}$$

$$a_{14b} = -\frac{L_{adpp} i_{q0}}{2HL_{fd}} + K_{d4b}\left(\frac{\varphi_{aq}}{2H} + \frac{L_{adpp} i_{q0}}{2H}\right)$$

$$a_{15b} = -\frac{L_{adpp} i_{q0}}{2HL_{1d}} + K_{d5b}\left(\frac{\varphi_{aq}}{2H} + \frac{L_{adpp} i_{q0}}{2H}\right)$$

$$a_{16b} = K_{q6b}\left(-\frac{\varphi_{ad}}{2H} - \frac{L_{aqpp} i_{d0}}{2H}\right)$$

$$a_{17b} = \frac{L_{aqpp} i_{d0}}{2HL_{1q}} + K_{q7b}\left(-\frac{\varphi_{ad}}{2H} - \frac{L_{aqpp} i_{d0}}{2H}\right)$$

$$a_{18b} = \frac{L_{aqpp} i_{d0}}{2HL_{2q}} + K_{q8b}\left(-\frac{\varphi_{ad}}{2H} - \frac{L_{aqpp} i_{d0}}{2H}\right)$$

$$a_{21b} = \omega_0$$

$$a_{33b} = \omega_0 R_a K_{d3b}$$

$$a_{34b} = \omega_0 R_a K_{d4b}$$

$$a_{35b} = \omega_0 R_a K_{d5b}$$

$$a_{36b} = \omega_0$$

$$a_{43b} = -K_{d3b}\frac{\omega_0 R_{fd} L_{adpp}}{L_{fd}}$$

$$a_{44b} = \left(-\frac{\omega_0 R_{fd}}{L_{fd}} + \frac{\omega_0 R_{fd} L_{adpp}}{L_{fd}^2}\right) -$$

$$K_{d4b}\frac{\omega_0 R_{fd} L_{adpp}}{L_{fd}}$$

$$a_{45b} = \frac{\omega_0 R_{fd} L_{adpp}}{L_{fd} L_{1d}} - K_{d5b}\frac{\omega_0 R_{fd} L_{adpp}}{L_{fd}}$$

$$a_{55b} = \left(-\frac{\omega_0 R_{1d}}{L_{1d}} + \frac{\omega_0 R_{1d} L_{adpp}}{L_{1d}^2}\right) - K_{d5b}\frac{\omega_0 R_{1d} L_{adpp}}{L_{1d}}$$

$$a_{63b} = \omega_0$$

$$a_{66b} = \omega_0 R_a K_{q6b}$$

$$a_{67b} = \omega_0 R_a K_{q7b}$$

$$a_{68b} = \omega_0 R_a K_{q8b}$$

$$a_{76b} = -K_{q6b}\frac{\omega_0 R_{1q} L_{aqpp}}{L_{1q}}$$

$$a_{77b} = \left(-\frac{\omega_0 R_{1q}}{L_{1q}} + \frac{\omega_0 R_{1q} L_{aqpp}}{L_{1q}^2}\right) - K_{q7b}\frac{\omega_0 R_{1q} L_{aqpp}}{L_{1q}}$$

$$a_{78b} = \frac{\omega_0 R_{1q} L_{aqpp}}{L_{1q} L_{2q}} - K_{q8b}\frac{\omega_0 R_{1q} L_{aqpp}}{L_{1q}}$$

$$a_{86b} = -K_{q6b}\frac{\omega_0 R_{2q} L_{aqpp}}{L_{2q}}$$

$$a_{87b} = \frac{\omega_0 R_{2q} L_{aqpp}}{L_{2q} L_{1q}} - K_{q7b}\frac{\omega_0 R_{2q} L_{aqpp}}{L_{2q}}$$

$$a_{88b} = \left(-\frac{\omega_0 R_{2q}}{L_{2q}} + \frac{\omega_0 R_{2q} L_{aqpp}}{L_{2q}^2}\right) - K_{q8b}\frac{\omega_0 R_{2q} L_{aqpp}}{L_{2q}}$$

The parameters of the $B_{gb}$ matrix is given by,

$$b_{11b} = \frac{1}{2H}$$

$$b_{42b} = \frac{\omega_0 R_{fd}}{L_{ad}}$$

The parameters of the $D_{gb}$ matrix are given by,

$$d_{31b} = \omega_0$$

$$d_{62b} = \omega_0$$

### 4.1.3. Network model

Network of the selected bench mark model has series compensated transmission line as shown in figure 4.7. This network model should represent using dynamic phasor model to eliminate $e_d$ and $e_q$ in equation 4.20 which are d and q components of the terminal voltage of the generator ($E_t$). Equations for the network using dynamic phasor model are shown in equation 4.21 and 4.22.

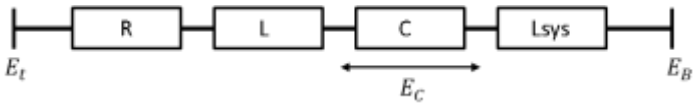


*Figure 4.7: Series compensated transmission line*

$$E_{t(RI)} - E_{B(RI)} = RI_{(RI)} + \left(X_L + X_{sys}\right)\frac{dI_{(RI)}}{dt} + E_{C(RI)} \quad 4.21$$

$$\frac{dE_{C(RI)}}{dt} = \frac{1}{X_C} I_{(RI)} \quad 4.22$$

Where,

$E_{B(RI)} = E_{BR} + jE_{BI}$

$E_{t(RI)} = E_{tR} + jE_{tI}$

$E_{C(RI)} = E_{CR} + jE_{CI}$

$I_{(RI)} = I_R + jI_I$

Equation 4.21 and 4.22 are written by taking a reference frame which is known as "R-I" frame. Those equations should transformed into "d-q" frame to substitute $e_d$ and $e_q$ in equation 4.16 and 4.17. The transformation from common reference frame to machine d-q frame is shown in figure 4.8. The relationship between the quantities in "d-q" frame and "R-I" frame is given by the equation 4.23 and 4.24.

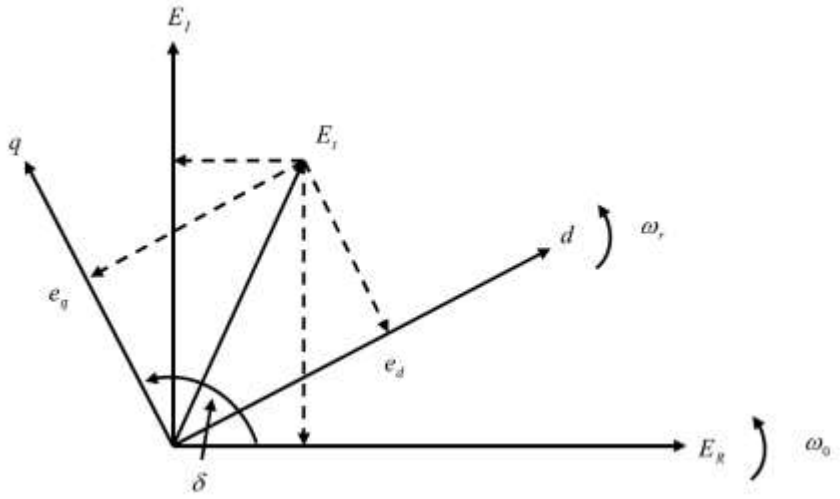


*Figure 4.8: transformation from common reference frame to machine d-q frame*

$$\begin{bmatrix} e_q \\ e_d \end{bmatrix} = \begin{bmatrix} cos\delta & sin\delta \\ sin\delta & -cos\delta \end{bmatrix} \begin{bmatrix} E_R \\ E_I \end{bmatrix} \quad 4.23$$

$$\begin{bmatrix} i_q \\ i_d \end{bmatrix} = \begin{bmatrix} cos\delta & sin\delta \\ sin\delta & -cos\delta \end{bmatrix} \begin{bmatrix} I_R \\ I_I \end{bmatrix} \quad 4.24$$

Take, $\begin{bmatrix} cos\delta & sin\delta \\ sin\delta & -cos\delta \end{bmatrix} = K = K^{-1}$

$$\begin{bmatrix} -sin\delta & cos\delta \\ cos\delta & sin\delta \end{bmatrix} = \dot{K}$$

Then equation 4.23 and 4.24 can multiply by K to transform them into d-q frame as given by equations 4.25 and 4.26.

$$KE_{t(RI)} - KE_{B(RI)} = RKI_{(RI)} + (X_L + X_{sys})K\frac{dI_{(RI)}}{dt} + KE_{C(RI)} \quad 4.25$$

$$K\frac{dE_{C(RI)}}{dt} = \frac{1}{X_C}KI_{(RI)} \quad 4.26$$

Equation 4.25 and 4.26 can be written as given in equation 4.27 and 4.28.

$$E_{t(qd)} - E_{B(qd)} = RI_{(qd)} + \left(X_L + X_{sys}\right)K\frac{dK^{-1}I_{(qd)}}{dt} + E_{C(qd)} \quad 4.27$$

$$K\frac{dK^{-1}E_{C(qd)}}{dt} = \frac{1}{X_C}I_{(qd)} \quad 4.28$$

By simplify equation 4.27 and 4.28, q and d components of the equations can be given as in equation 4.29 to 4.32.

$$e_q - E_{Bq} = RI_q + \left(X_L + X_{sys}\right)\left[\dot{I_q} + I_d\omega_r\right] + E_{Cq} \quad 4.29$$

$$e_d - E_{Bd} = RI_d + \left(X_L + X_{sys}\right)\left[\dot{I_d} - I_q\omega_r\right] + E_{Cd} \quad 4.30$$

$$\dot{E_{Cq}} = \frac{1}{X_C}I_q - E_{Cd}\omega_r \quad 4.31$$

$$\dot{E_{Cd}} = \frac{1}{X_C}I_d + E_{Cq}\omega_r \quad 4.32$$

Where,

$E_{Bq} = E_B cos\delta$ and $E_{Bd} = E_B sin\delta$

After linearizing equations 4.29 to 4.32 and substitute $\dot{I_q}$ and $\dot{I_d}$ from equations 4.14, 4.15 and 4.24, $\Delta\dot{\varphi}_q$ and $\Delta\dot{\varphi}_d$ can be given as in equation 4.33 and 4.34. Two components of the voltage across the capacitor is given by equation 4.35 and 4.36.

$$\begin{aligned}\Delta\dot{\varphi}_q = {} & a_{61b1}\Delta\omega_r + a_{62b1}\Delta\delta + a_{63b1}\Delta\varphi_d + a_{64b1}\Delta\varphi_{fd} + a_{65b1}\Delta\varphi_{1d} \\ & + a_{66b1}\Delta\varphi_q + a_{67b1}\Delta\varphi_{1q} + a_{68b1}\Delta\varphi_{2q} + a_{69b1}\Delta E_{cq}\end{aligned} \quad 4.33$$

$$\begin{aligned}\Delta\dot{\varphi}_d = {} & a_{31b1}\Delta\omega_r + a_{32b1}\Delta\delta + a_{33b1}\Delta\varphi_d + a_{34b1}\Delta\varphi_{fd} + a_{35b1}\Delta\varphi_{1d} \\ & + a_{36b1}\Delta\varphi_q + a_{37b1}\Delta\varphi_{1q} + a_{38b1}\Delta\varphi_{2q} + a_{310b1}\Delta E_{cd} \\ & + b_{32b1}\Delta E_{fd}\end{aligned} \quad 4.34$$

$$\Delta\dot{E}_{cq} = a_{91b1}\Delta\omega_r + a_{96b1}\Delta\varphi_q + a_{97b1}\Delta\varphi_{1q} + a_{98b1}\Delta\varphi_{2q} + a_{910b1}\Delta E_{cd} \quad 4.35$$

$$\Delta\dot{E}_{cd} = a_{101b1}\Delta\omega_r + a_{103b1}\Delta\varphi_d + a_{104b1}\Delta\varphi_{fd} + a_{105b1}\Delta\varphi_{1d} + a_{109b1}\Delta E_{cq} \quad 4.36$$

Where,

$a_{61b1} = \omega_0(X_L + X_{sys})i_{d0}/(1 + \omega_0(X_L + X_{sys})K_{q6b})$

$a_{62b1} = \omega_0 E_B \cos(\delta)/(1 + \omega_0(X_L + X_{sys})K_{q6b})$

$a_{63b1} = [\omega_0(X_L + X_{sys})K_{d3b} + a_{63b}]/(1 + \omega_0(X_L + X_{sys})K_{q6b})$

$a_{64b1} = \omega_0(X_L + X_{sys})K_{d4b}/(1 + \omega_0(X_L + X_{sys})K_{q6b})$

$a_{65b1} = \omega_0(X_L + X_{sys})K_{d5b}/(1 + \omega_0(X_L + X_{sys})K_{q6b})$

$a_{65b1} = \{\omega_0(X_L + X_{sys})(K_{q7b}a_{76b} + K_{q8b}a_{86b}) + a_{66b} + \omega_0 K_{q6b}R\}/(1 + \omega_0(X_L + X_{sys})K_{q6b})$

$a_{67b1} = \{\omega_0(X_L + X_{sys})(K_{q7b}a_{77b} + K_{q8b}a_{87b}) + a_{67b} + \omega_0 K_{q7b}R\}/(1 + \omega_0(X_L + X_{sys})K_{q6b})$

$a_{68b1} = \{\omega_0(X_L + X_{sys})(K_{q7b}a_{78b} + K_{q8b}a_{88b}) + a_{68b} + \omega_0 K_{q8b}R\}/(1 + \omega_0(X_L + X_{sys})K_{q6b})$

$a_{69b1} = \omega_0/(1 + \omega_0(X_L + X_{sys})K_{q6b})$

$a_{31b1} = -\omega_0(X_L + X_{sys})i_{q0}/(1 + \omega_0(X_L + X_{sys})K_{d3b})$

$a_{32b1} = -\omega_0 E_B \sin\delta)/(1 + \omega_0(X_L + X_{sys})K_{d3b})$

$a_{33b1} = \{\omega_0(X_L + X_{sys})(K_{d4b}a_{43b} + K_{d5b}a_{53b}) + a_{33b} + \omega_0 K_{d3b}R\}/(1 + \omega_0(X_L + X_{sys})K_{d3b})$

$$a_{34b1} = \{\omega_0(X_L + X_{sys})(K_{d4b}a_{44b} + K_{d5b}a_{54b}) + a_{34b} + \omega_0 K_{d4b}R\}/(1 + \omega_0(X_L + X_{sys})K_{d3b})$$

$$a_{35b1} = \{\omega_0(X_L + X_{sys})(K_{d4b}a_{45b} + K_{d5b}a_{55b}) + a_{35b} + \omega_0 K_{d5b}R\}/(1 + \omega_0(X_L + X_{sys})K_{d3b})$$

$$a_{36b1} = [-\omega_0(X_L + X_{sys})K_{q6b} + a_{36b}]/(1 + \omega_0(X_L + X_{sys})K_{d3b})$$

$$a_{37b1} = -\omega_0(X_L + X_{sys})K_{q7b}/(1 + \omega_0(X_L + X_{sys})K_{d3b})$$

$$a_{38b1} = -\omega_0(X_L + X_{sys})K_{q8b}/(1 + \omega_0(X_L + X_{sys})K_{d3b})$$

$$a_{310b1} = \omega_0/(1 + \omega_0(X_L + X_{sys})K_{d3b})$$

$$b_{32b1} = \omega_0(X_L + X_{sys})K_{d4b}b_{42b}/(1 + \omega_0(X_L + X_{sys})K_{d3b})$$

$$a_{91b1} = -E_{cd0}$$

$$a_{96b1} = K_{q6b}/X_C$$

$$a_{97b1} = K_{q7b}/X_C$$

$$a_{98b1} = K_{q8b}/X_C$$

$$a_{910b1} = -1$$

$$a_{101b1} = E_{cq0}$$

$$a_{103b1} = K_{d3b}/X_C$$

$$a_{104b1} = K_{d4b}/X_C$$

$$a_{105b1} = K_{d5b}/X_C$$

$$a_{109b1} = 1$$

### 4.1.4. Generator and network model

Combination of generator model and network model can be derived by eliminating $\Delta e_d$ and $\Delta e_q$ of equation 4.20 using equation 4.33 and 4.34. d-q components of the capacitor voltage are considered as state variables. The 10$^{th}$ order combined state space model is given by equation 4.37. The model is given in the form of $\Delta \dot{X}_g = A_g \Delta X_g + B_g \Delta U_g$. There are 10 state variables, rotor speed ($\omega_r$), rotor angle ($\delta$), flux of the d-axis stator winding ($\varphi_d$), flux of the d-axis field winding ($\varphi_{fd}$), flux of the damper winding of d-axis ($\varphi_{1d}$), flux of the q-axis stator winding ($\varphi_q$), flux of the q-axis first damper winding ($\varphi_{1q}$), flux of the q-axis second damper winding ($\varphi_{2q}$) , d component of capacitor voltage ($E_{cd}$) and q component of capacitor voltage ($E_{cq}$) and two inputs: mechanical torque ($T_m$) and voltage applied to the field winding ($E_{fd}$) in the system.

$$\begin{bmatrix} \Delta\dot{\omega}_r \\ \Delta\dot{\delta} \\ \Delta\dot{\varphi}_d \\ \Delta\dot{\varphi}_{fd} \\ \Delta\dot{\varphi}_{1d} \\ \Delta\dot{\varphi}_q \\ \Delta\dot{\varphi}_{1q} \\ \Delta\dot{\varphi}_{2q} \\ \Delta\dot{E}_{cq} \\ \Delta\dot{E}_{cd} \end{bmatrix} = \begin{bmatrix} a_{11b} & 0 & a_{13b} & a_{14b} & a_{15b} & a_{16b} & a_{17b} & a_{18b} & 0 & 0 \\ a_{21b} & 0 & 0 & 0 & 0 & 0 & 0 & 0 & 0 & 0 \\ a_{31b1} & a_{32b1} & a_{33b1} & a_{34b1} & a_{35b1} & a_{36b1} & a_{37b1} & a_{38b1} & 0 & a_{310b1} \\ 0 & 0 & a_{43b} & a_{44b} & a_{45b} & 0 & 0 & 0 & 0 & 0 \\ 0 & 0 & a_{53b} & a_{54b} & a_{55b} & 0 & 0 & 0 & 0 & 0 \\ a_{61b1} & a_{62b1} & a_{63b1} & a_{64b1} & a_{65b1} & a_{66b1} & a_{67b1} & a_{68b1} & a_{69b1} & 0 \\ 0 & 0 & 0 & 0 & 0 & a_{76b} & a_{77b} & a_{78b} & 0 & 0 \\ 0 & 0 & 0 & 0 & 0 & a_{86b} & a_{87b} & a_{88b} & 0 & 0 \\ a_{91b1} & 0 & 0 & 0 & 0 & a_{96b1} & a_{97b1} & a_{98b1} & 0 & a_{910b1} \\ a_{101b1} & 0 & a_{103b1} & a_{104b1} & a_{105b1} & 0 & 0 & 0 & a_{109b1} & 0 \end{bmatrix} \begin{bmatrix} \Delta\omega_r \\ \Delta\delta \\ \Delta\varphi_d \\ \Delta\varphi_{fd} \\ \Delta\varphi_{1d} \\ \Delta\varphi_q \\ \Delta\varphi_{1q} \\ \Delta\varphi_{2q} \\ \Delta E_{cq} \\ \Delta E_{cd} \end{bmatrix} + \begin{bmatrix} b_{11b} & 0 \\ 0 & 0 \\ 0 & b_{32b1} \\ 0 & b_{42b} \\ 0 & 0 \\ 0 & 0 \\ 0 & 0 \\ 0 & 0 \\ 0 & 0 \\ 0 & 0 \end{bmatrix} \begin{bmatrix} \Delta T_m \\ \Delta E_{fd} \end{bmatrix} \qquad 4.37$$

### 4.1.5. Multi-mass turbine model

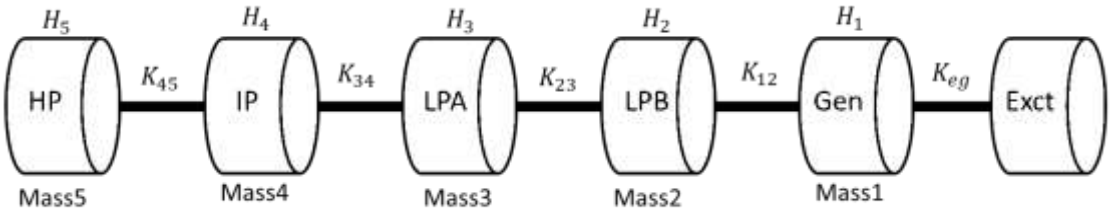


*Figure 4.9: The multi mass turbine model*

The multi mass turbine model with four turbines (High pressure, Intermediate pressure, Low pressure A and Low pressure B), generator and exciter shown in figure 4.9 is used in the analysis. The speed and the rotor angle of each mass unit are selected as state variables. The dynamic equations of the speed and the rotor angle of each mass unit are given by equations 4.38 and 4.39.

$$2H_i\Delta\dot{\omega}_\iota = K_{i,i+1}(\Delta\delta_{i+1} - \Delta\delta_i) - K_{i-1,i}(\Delta\delta_i - \Delta\delta_{i-1}) - K_{di}\Delta\omega_i + \Delta T_i \qquad 4.38$$

$$\Delta\dot{\delta_\iota} = \omega_0\,\Delta\omega_i \qquad 4.39$$

Where,

$K_{i,j}$ represents the spring constant between i$^{th}$ mass and j$^{th}$ mass

$H_i$ represents the inertia constant of i$^{th}$ mass

$K_{di}$ represents the damping coefficient of i$^{th}$ mass

$T_i$ represents the torque generated by i$^{th}$ mass

### 4.1.6. Overall state space model.

The 20th order overall state space model is given by equation 4.40. The model is given in the form of $\Delta\dot{X} = A_{sys}\Delta X + B_{sys}\Delta U$. There are 20 state variables, rotor speed ($\omega_r$), rotor angle ($\delta$), flux of the d-axis stator winding ($\varphi_d$), flux of the d-axis field winding ($\varphi_{fd}$), flux of the damper winding of d-axis ($\varphi_{1d}$), flux of the q-axis stator winding ($\varphi_q$), flux of the q-axis first damper winding ($\varphi_{1q}$), flux of the q-axis second damper winding ($\varphi_{2q}$) , d component of capacitor voltage ($E_{cd}$), q component of capacitor voltage ($E_{cq}$), rotor speed of LPB turbine ($\omega_2$), rotor angle of LPB turbine ($\delta_2$), rotor speed of LPA turbine ($\omega_3$), rotor angle of LPA turbine ($\delta_3$), rotor speed of IP turbine ($\omega_4$), rotor angle of IP turbine ($\delta_4$), rotor speed of HP turbine ($\omega_5$), rotor angle of HP turbine ($\delta_5$), rotor speed of the exciter mass ($\omega_e$) and rotor angle of the exciter mass ($\delta_e$), and two inputs: mechanical torque ($T_m$) and voltage applied to the field winding ($E_{fd}$) in the system.

For the analysis output of the overall system is taken as the rotor speed ($\omega_r$) and given by the equation 4.41. Output equation for the overall system is given in the form of $\Delta Y = C_{sys}\Delta X$.

$$\Delta\dot{X}_{20\times1} = A_{sys}{}_{20\times20}\Delta X_{20\times1} + B_{sys}{}_{20\times2}\Delta U_{2\times1} \qquad 4.40$$

Where,

$$\Delta X_{20\times1} = [\Delta\omega_r \quad \Delta\delta \quad \Delta\varphi_d \quad \Delta\varphi_{fd} \quad \Delta\varphi_{1d} \quad \Delta\varphi_q \quad \Delta\varphi_{1q} \quad \Delta\varphi_{2q} \quad \Delta E_{cq} \quad \Delta E_{cd} \quad \Delta\omega_2 \quad \Delta\delta_2 \quad \Delta\omega_3 \quad \Delta\delta_3 \quad \Delta\omega_4 \quad \Delta\delta_4 \quad \Delta\omega_5 \quad \Delta\delta_5 \quad \Delta\omega_e \quad \Delta\delta_e]^T$$

$$B_{sys_{20\times2}} = \begin{bmatrix} b_{11b} & 0 & 0 & 0 & 0 & 0 & 0 & 0 & 0 & b_{111b} & 0 & b_{131b} & 0 & b_{151b} & 0 & b_{171b} & 0 & 0 & 0 \\ 0 & 0 & b_{32b} & b_{42b} & 0 & 0 & 0 & 0 & 0 & 0 & 0 & 0 & 0 & 0 & 0 & 0 & 0 & 0 & 0 \end{bmatrix}^T$$

$$\Delta U_{2\times1} = \begin{bmatrix} \Delta T_m \\ \Delta E_{fd} \end{bmatrix}$$

$$A_{sys_{20\times20}}$$

$$= \begin{bmatrix}
a_{11b} & 0 & a_{13b} & a_{14b} & a_{15b} & a_{16b} & a_{17b} & a_{18b1} & 0 & 0 & 0 & a_{112b1} & 0 & 0 & 0 & 0 & 0 & 0 & 0 & a_{120b1} \\
a_{21b} & 0 & 0 & 0 & 0 & 0 & 0 & 0 & 0 & 0 & 0 & 0 & 0 & 0 & 0 & 0 & 0 & 0 & 0 & 0 \\
a_{31b1} & a_{32b1} & a_{33b1} & a_{34b1} & a_{35b1} & a_{36b1} & a_{37b1} & a_{38b1} & 0 & a_{310b1} & 0 & 0 & 0 & 0 & 0 & 0 & 0 & 0 & 0 & 0 \\
0 & 0 & a_{43b} & a_{44b} & a_{45b} & 0 & 0 & 0 & 0 & 0 & 0 & 0 & 0 & 0 & 0 & 0 & 0 & 0 & 0 & 0 \\
0 & 0 & a_{53b} & a_{54b} & a_{55b} & 0 & 0 & 0 & 0 & 0 & 0 & 0 & 0 & 0 & 0 & 0 & 0 & 0 & 0 & 0 \\
a_{61b1} & a_{62b1} & a_{63b1} & a_{64b1} & a_{65b1} & a_{66b1} & a_{67b1} & a_{68b1} & a_{69b1} & 0 & 0 & 0 & 0 & 0 & 0 & 0 & 0 & 0 & 0 & 0 \\
0 & 0 & 0 & 0 & 0 & a_{76b} & a_{77b} & a_{78b} & 0 & 0 & 0 & 0 & 0 & 0 & 0 & 0 & 0 & 0 & 0 & 0 \\
0 & 0 & 0 & 0 & 0 & a_{86b} & a_{87b} & a_{88b} & 0 & 0 & 0 & 0 & 0 & 0 & 0 & 0 & 0 & 0 & 0 & 0 \\
a_{91b1} & 0 & 0 & 0 & 0 & a_{96b1} & a_{97b1} & a_{98b1} & 0 & a_{910b1} & 0 & 0 & 0 & 0 & 0 & 0 & 0 & 0 & 0 & 0 \\
a_{101b1} & 0 & a_{103b1} & a_{104b1} & a_{105b1} & 0 & 0 & 0 & a_{109b1} & 0 & 0 & 0 & 0 & 0 & 0 & 0 & 0 & 0 & 0 & 0 \\
0 & a_{112b} & 0 & 0 & 0 & 0 & 0 & 0 & 0 & 0 & a_{1111b} & a_{1112b} & 0 & a_{1114b} & 0 & 0 & 0 & 0 & 0 & 0 \\
0 & 0 & 0 & 0 & 0 & 0 & 0 & 0 & 0 & 0 & a_{1211b} & 0 & 0 & 0 & 0 & 0 & 0 & 0 & 0 & 0 \\
0 & 0 & 0 & 0 & 0 & 0 & 0 & 0 & 0 & 0 & 0 & a_{1312b} & a_{1313b} & a_{1314b} & 0 & a_{1316b} & 0 & 0 & 0 & 0 \\
0 & 0 & 0 & 0 & 0 & 0 & 0 & 0 & 0 & 0 & 0 & 0 & a_{1413b} & 0 & 0 & 0 & 0 & 0 & 0 & 0 \\
0 & 0 & 0 & 0 & 0 & 0 & 0 & 0 & 0 & 0 & 0 & 0 & 0 & a_{1514b} & a_{1515b} & a_{1516b} & 0 & a_{1518b} & 0 & 0 \\
0 & 0 & 0 & 0 & 0 & 0 & 0 & 0 & 0 & 0 & 0 & 0 & 0 & 0 & a_{1615b} & 0 & 0 & 0 & 0 & 0 \\
0 & 0 & 0 & 0 & 0 & 0 & 0 & 0 & 0 & 0 & 0 & 0 & 0 & 0 & 0 & a_{1716b} & a_{1717b} & a_{1718b} & 0 & 0 \\
0 & 0 & 0 & 0 & 0 & 0 & 0 & 0 & 0 & 0 & 0 & 0 & 0 & 0 & 0 & 0 & a_{1817b} & 0 & 0 & 0 \\
0 & a_{192b} & 0 & 0 & 0 & 0 & 0 & 0 & 0 & 0 & 0 & 0 & 0 & 0 & 0 & 0 & 0 & 0 & a_{1919b} & a_{1920b} \\
0 & 0 & 0 & 0 & 0 & 0 & 0 & 0 & 0 & 0 & 0 & 0 & 0 & 0 & 0 & 0 & 0 & 0 & a_{2019b} & 0
\end{bmatrix}$$

New parameters of matrix $A_{sys}{}_{20\times20}$ are given by,

$a_{112b1} = K_{12}/2H_1$

$a_{120b1} = K_{01}/2H_1$

$a_{112b} = K_{12}/2H_2$

$a_{1111b} = -K_{d2}/2H_2$

$a_{1112b} = -(K_{23} + K_{12})/2H_2$

$a_{1114b} = K_{23}/2H_2$

$a_{1211b} = \omega_0$

$a_{1312b} = K_{23}/2H_3$

$a_{1313b} = -K_{d3}/2H_3$

$a_{1314b} = -(K_{34} + K_{23})/2H_3$

$a_{1316b} = K_{34}/2H_3$

$a_{1413b} = \omega_0$

$a_{1514b} = K_{34}/2H_4$

$a_{1515b} = -K_{d4}/2H_4$

$a_{1516b} = -(K_{45} + K_{34})/2H_4$

$a_{1518b} = K_{45}/2H_4$

$a_{1615b} = \omega_0$

$a_{1716b} = K_{45}/2H_5$

$a_{1717b} = -K_{d5}/2H_5$

$a_{1718b} = -K_{45}/2H_5$

$a_{1817b} = \omega_0$

$a_{192b} = K_{01}/2H_e$

$a_{1919b} = -K_{d0}/2H_e$

$a_{1920b} = -K_{01}/2H_e$

$a_{2019b} = \omega_0$

New parameters of matrix $B_{sys}{}_{20\times2}$ are given by,

$b_{111b} = 0.22/2H_2$

$b_{131b} = 0.22/2H_3$

$b_{151b} = 0.26/2H_4$

$b_{171b} = 0.3/2H_5$

$$\Delta Y_{1\times1} = C_{sys}{}_{1\times20}\Delta X_{20\times1} \qquad 4.41$$

Where,

$$C_{sys_{1\times 20}} = [1 \quad 0 \quad 0 \quad 0 \quad 0 \quad 0 \quad 0 \quad 0 \quad 0 \quad 0 \quad 0 \quad 0 \quad 0 \quad 0 \quad 0 \quad 0 \quad 0 \quad 0 \quad 0 \quad 0]$$

## 4.2. Inceptive conditions of the state variables of the selected power system

The inceptive conditions (the values at steady state condition) of the state variables of the selected system are derived by solving some algebraic equations as given below. In power system studies, a power flow analysis is conducted to recognize the operating point. For this analysis the outputs that gives the active power (P), reactive power (Q), angle of the voltage (θ) and magnitude of the voltage (V) at individual bus together with the generator bus are used. This is the preliminary point for the initial condition calculation of the state variables.

For this test system, the armature current ($I_a$) of the synchronous generator can be calculated from the equation 4.42 and the voltage behind $X_q$, ($e_q \angle \delta$) can be calculated by using equation 4.43.

$$I_a \angle \emptyset = \frac{P_g - jQ_g}{V_g \angle \theta_g} \tag{4.42}$$

$$e_q \angle \delta = V_g \angle \theta_g + (R_a + jX_q) I_a \angle \emptyset \tag{4.43}$$

Then other initial values of the state variables which are required for the calculations, can be derived by using equations 4.44 to 4.53.

$$i_d = -I_a \sin(\delta - \emptyset) \tag{4.44}$$

$$i_q = I_a \cos(\delta - \emptyset) \tag{4.45}$$

$$v_d = -V_g \sin(\delta - \theta_g) \tag{4.46}$$

$$v_q = V_g \cos(\delta - \theta_g) \tag{4.47}$$

$$E_{fd} = E_q - (X_d - X_q)i_d \quad 4.48$$

$$\varphi_d = X_d i_d + E_{fd} \quad 4.49$$

$$\varphi_q = X_q i_q \quad 4.50$$

$$\varphi_{fd} = \varphi_d + \frac{X_{dp}}{X_d - X_{dp}} E_{fd} \quad 4.51$$

$$\varphi_{1d} = \varphi_d \quad 4.52$$

$$\varphi_{1q} = \varphi_{2q} = \varphi_q \quad 4.53$$

The values of the state variables of the test system at the steady state condition is given by table 4.3.

*Table 4.4: Values of state variables at steady state condition*

| | | | |
|---|---|---|---|
| $i_d$ | 0.9639 | $\varphi_d$ | 2.5721 |
| $i_q$ | 0.1972 | $\varphi_q$ | 0.3372 |
| $v_d$ | 0.4779 | $\varphi_{fd}$ | 2.6604 |
| $v_q$ | 0.8784 | $\varphi_{1d}$ | 2.5721 |
| $E_{fd}$ | 0.8466 | $\varphi_{1q}, \varphi_{2q}$ | 0.3372 |

## 4.3. Eigenvalue analysis for the test system

The overall state space representation of the linearized system (multi-mass model, generator model and network model) has the form $\Delta\dot{X} = A_{sys}\Delta X + B_{sys}\Delta U$. This system is 20$^{th}$ order system and there should be 20 eigenvalues. The eigenvalues ($\lambda_{sys}$) of this linear system can be derived by the matrix equation shown in equation 4.54.

$$\det[\lambda_{sys} I - A_{sys}] = 0 \qquad 4.54$$

Linearized overall system is coded using MATLAB software to derive matrix $A_{sys}$ and matrix $B_{sys}$ and using equation 4.54, eigenvalues of the system under 80 % of series capacitor compensation was found as given in Table 4.4.

*Table 4.5: Eigenvalues of the system under 80 % of series capacitor compensation*

| Number of the eigenvalue | Real part | Imaginary part | Imaginary part (Hz) |
|---|---|---|---|
| 1,2 | -0.36 | ±298.16 | ±47.43 |
| 3,4 | -0.12 | ±202.84 | ±32.28 |
| 5,6 | -0. 35 | ±160.50 | ±25.46 |
| 7 | -34.8 | 0 | 0 |
| 8,9 | -1.32 | ±126.93 | ±20.20 |
| 10,11 | 0.35 | ±98.72 | ±15.71 |
| 12,13 | -9.34 | ±110.97 | ±17.66 |
| 14,15 | -1.32 | ±40.70 | ±6.48 |
| 16 | -19.39 | 0 | 0 |
| 17 | -1.98 | 0 | 0 |
| 18 | -0.03 | 0 | 0 |
| 19,20 | -0.27 | ±0 | ±0 |

From the table 4.4, it's clear that two eigenvalues of the power system are on the right-hand side from the imaginary axis and some eigenvalues have frequencies in sub-synchronous range. Hence, the system is not stable at the considered operating point of the system. The linear model of the same system has been derived in reference [18] for SSR studies and it is shown there the system is unstable at 70 % of compensation level.

## 4.4. Model verification

The test system was linearized by ignoring all the higher order terms of the 20th order system using Taylor series. Hence, final linearized model should be checked for the validation and the frequencies of the system were considered for this validation. The linearized model is validated by applying 1% disturbance on the system input, $E_{fd}$. For the inputs, Tm and $E_{fd}$, the speed variation of the linearized model was compared with the non-linearized model which was developed using PSCAD. Figure 4.10 shows the speed variations of the linearized small signal model and the non-linearized model.

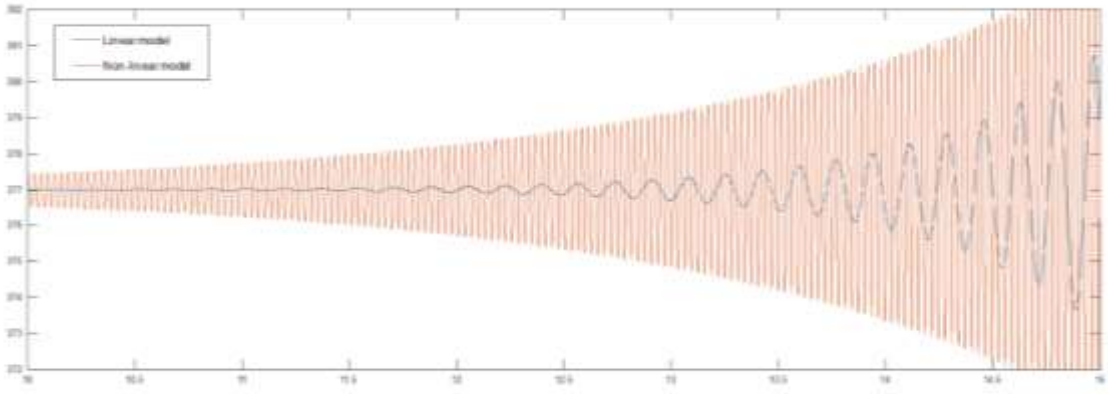

*Figure 4.10: Speed variation of linear and nonlinear models*

Further, to analyze the frequencies of the system FFT analysis tool in MATLAB software was used. Linearized model was coded in MALTAB software itself and the original non-linear system was simulated using PSCAD software and data of the output waveform were

transfer to the MATLAB software for FFT analysis. It was proved the frequency range of the linearized system is coherence with the frequency range of the original system. Results from FFT analysis tool for the non-linearized model is given in Figure 4.11. Frequencies of the Linearized model derived by the eigenvalues, were compared with the frequencies of the non-linearized model in Table 4.6.

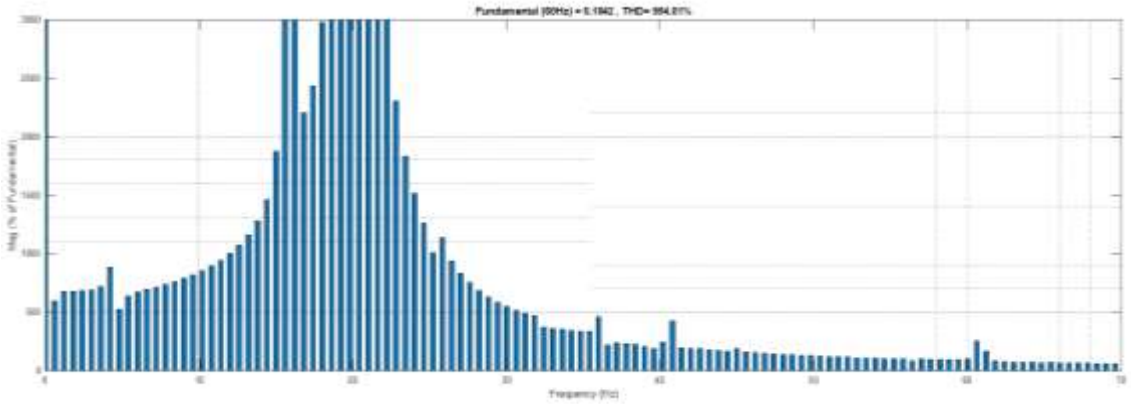

*Figure 4.111: FFT for non-linear model*

*Table 4.6: Frequency Comparison of the Linear and Non-linear Models*

| Frequencies of linear model | Frequencies of non-linear model |
|---|---|
| 47.43 | 47.4 |
| 32.28 | 32.4 |
| 25.46 | 25.2 |
| 20.20 | 20.4 |
| 15.71 | 15.6 |
| 17.66 | 17.4 |
| 6.48 | 6.6 |

# CHAPTER 05

# DESIGNING THE CONTROLLER

In the previous section all the calculations were done for only one operating point of the test system, 70% of series compensation. Controller is designed to perform well on different operating points by changing the compensation percentage. Hence, value of the capacitor in the linear model is set to be varied when designing the controller.

A PID controller was designed for this multi-input linearized test system and rotor speed was taken as the output of the system. Since, this test system is an unstable system, to select the inceptive values of P, I and D controller parameters, Ziegler Nichols (Z-N) method is used for separate inputs with consider only one operating point (80% series compensation). Then, simulated annealing method was used as the optimization method to optimize the controller to perform well under different operating points.

## 5.1. Ziegler Nichols (Z-N) method

The Ziegler–Nichols method practices to tune a PID controller and this is known as an experimental method which starts the performance by keeping the derivative (D) and integral (I) gains to zero. The ultimate gain, $K_u$ can be derived by increasing the proportional (P) gain, $K_P$ from zero until the control loop output has consistent and stable oscillation. Ultimate gain, $K_u$ and the period of oscillation, $T_u$ are used to derive the P, I, and D controller gains which are dependent on the controller type used. Setting of P, I, and D gains with the controller type is shown in table5.1.

*Table 5.1: Setting of P, I, and D gains with the controller type*

| Type of the control | $K_P$ | $T_i$ | $T_d$ | $K_i$ | $K_d$ |
|---|---|---|---|---|---|

| | | | | | |
|---|---|---|---|---|---|
| P | $0.5K_u$ | - | - | - | - |
| PI | $0.45K_u$ | $T_u / 1.2$ | - | $0.54K_u / T_u$ | - |
| PD | $0.8K_u$ | - | $T_u / 8$ | - | $K_u T_u / 10$ |
| PID | $0.6K_u$ | $T_u / 2$ | $T_u / 8$ | $1.2K_u / T_u$ | $3K_u T_u / 40$ |

This method can only use for single input single output systems. Hence, the two inputs, mechanical torque of the synchronous generator ($T_m$) and voltage given to the field winding of the generator ($E_{fd}$), were separately selected to guess the initial parameters of PID the controller on 80% series compensation of the test system. To find $K_u$ and $T_u$ values, "Control System Designer" toolbox in MATLAB software was used. $K_u$ and $T_u$ values and initial P, I and D gains are given in the table 5.2.

*Table 5.2: $K_u$ and $T_u$ values and initial P, I and D gains*

| Input | $K_u$ | $T_u$ | $K_P$ | $T_i$ | $T_d$ | $K_i$ | $K_d$ |
|---|---|---|---|---|---|---|---|
| 1 ($T_m$) | 4.89 | 3.95 | 2.9 | 1.98 | 0.49 | 2.9 | 1.45 |
| 2 ($E_{fd}$) | 0.43 | 2.2 | 0.3 | 1.1 | 0.28 | 2.6 | 0.8 |

## 5.2. Simulated Annealing Method

Simulated annealing (SA) is an optimization technique and has been used in [19] to tune a frequency domain controller for Voltage Sourced Converter (VSC) systems. In this optimization method, the state of a physical system and the objective function which has to be minimized, is comparable with the total energy of the system in that state. The aim is to move the system from a random initial state to a state with the minimum possible energy.

The small signal model of the selected power system is derived by considering a specific operating point and the matrix $A_{sys}$ and $B_{sys}$ of the system depend on the operating point. By observing the eigenvalues of the state matrix ($A_{sys}$), stability of the system at a particular operating point can be decided. If all eigenvalues of the power system are on the left hand side of the complex plane, the particular system is said to be stable. For a particular operating point, the position of eigenvalues of the system can be affected by the controller gains. Hence, by considering the more than one operating point, effect of the controller gains on the stability of the overall system can be observed. Although the transient performance of a disturbance is typically controlled by the non-linearities such as non-linear gains and limits, the recovery of the system after a disturbance is determined by the eigenvalues of the system [19]. To achieve a better performance of the controller, all eigenvalues of the particular system should be on the left hand side of the complex plane and all oscillatory modes should be improved the damping for all selected operating points.

### 5.2.1. Objective function

The objective function use for the optimization is given in equation 5.1.

$$O = \sum_{n=1}^{N} \sum_{m=1}^{M} (P^{e(n,m)} + P^{d(n,m)}) \qquad 5.1$$

Where,

In the equation 5.1, M represents the number of eigenvalues of the system and N represents the number of selected operating points. $P^{e(n,m)}$ and $P^{d(n,m)}$ are to determine the penalty functions for eigenvalues and oscillation modes respectively.

$$P^{e(n,m)} = \begin{cases} 0 & if\ \xi_m \geq \xi_d \\ \xi_d - \xi_m & else \end{cases}$$

where, $\xi_d$ = desired location of the eigenvalue

$$P^{d(n,m)} = \begin{cases} 0 & if\ \sigma_m \leq \sigma_d \\ \sigma_m - \sigma_d & else \end{cases}$$

where, $\sigma_d$= desired damping value

In simulated annealing method, there are two loops, outer loop with iteration 1 (iter1) and inner loop with iteration 2 (iter2). According to equation 5.2, control parameter (C) is reduced at each iteration of the outer loop. The new solution can be accepted, when the objective function is reduced. When the objective function is raised, the Metropolis criteria, which is given in equation 5.3 is used to observe the acceptability of the new solution or otherwise, previous solution is stored as the current best solution.

$$C(iter_1) = K_C \times C(iter_1 - 1) \quad 5.2$$

where $K_C$ is a value close to and less than 1.

$$New\ solution = \begin{cases} accept & if\ e^{-\frac{\Delta O}{K_b C}} \geq rdm() \\ reject & else \end{cases} \quad 5.3$$

After the inner loop performed, $K_P$, $K_I$ *and* $K_d$ gain values are calculated using random numbers as give in equation 5.4 to 5.6. The optimization parameters are given in Table 5.3.

$$K_P(new) = K_P(old) + f_P * (rdm() - 0.5) \quad 5.4$$

$$K_I(new) = K_I(old) + f_I * (rdm() - 0.5) \quad 5.5$$

$$K_D(new) = K_D(old) + f_D * (rdm() - 0.5) \quad 5.6$$

Here, rdm() is an arbitrary value between 0 and 1. $f_P$ , $f_I$ and $f_D$ are assigned to measure the variations which are applied to the PID controller gains.

*Table 5.3: Optimization parameters*

| | | | |
|---|---|---|---|
| j | 20 | Iter1max | 1000 |
| i | 6 | $M_1$, $M_2$ | 30, 5 |
| fracP | 0.01 | C | 1 |
| fracI | 0.01 | $C_0$ | 0.001 |
| fracD | 0.01 | $K_C$ | 0.98 |

## 5.3. **Simulation results**

After applying the controller which was coded using MATLAB software, the values of the controller parameters were changed and table 5.4 shows the initial controller gain values and optimized controller gain values. The optimized controller gains were applied to the overall system as shown in Figure 5.2 by applying 1% disturbance on the system input, $E_{fd}$ with different line compensation levels separately. Table 5.5 shows the eigenvalues, oscillation frequency and damping factor of the overall controlled system in the sub-synchronous mode with different operating points. Six operating points were selected by changing the line compensation level from 30% to 80%. Reference [17] gives a comparative study of SSR characteristics of two FACTs controllers, TCSC and SSSC based on the analysis of IEEE first benchmark model with 40% of series capacitor compensation level. The eigen values of the system with designed PID controller with 40% compensation level and these two FACTS controllers are compare in Table 5.6. The corresponding eigen values are plotted in figure 5.1.

The designed PID controller was applied to the nonlinear model which was simulated on PSCAD software as shown in Figure 5.2. The simulation results for the output waveform (the generator speed waveform) of nonlinear model with and without the designed controller at different line compensation levels are shown in Figure 5.3 to 5.8. However, to tune the designed controller the exciter voltage ($E_{fd}$) have to change from a significant value and this can be mentioned as a limitation of the designed PID controller.

*Table 5.4: Initial values and optimized values of the controller gains*

| | Initial | Optimized |
|---|---|---|
| $K_P$ | 3.2 | 3.071 |
| $K_I$ | 5.5 | 5.649 |
| $K_D$ | 2.25 | 2.271 |

*Table5.5: Eigenvalues, oscillation frequency and damping factor of the overall controlled system in the sub-synchronous mode with different operating points*

| Compensation level | Without the controller | | | With the controller | | |
|---|---|---|---|---|---|---|
| | Eigenvalue | Frequency | Damping factor % | Eigenvalue | Frequency | Damping factor % |
| 30% | -0.12 ± 202.84i | 32.31 | 0.059 | -3.49 ± 203.31i | 32.31 | 1.72 |
| | -10.53 ± 199.51i | 31.83 | 5.27 | -11.63 ± 212.03i | 33.74 | 5.48 |
| | -0.35 ± 160.51i | 25.62 | 0.28 | -1 ± 177.83i | 28.33 | 0.56 |
| | -1.28 ± 126.93i | 20.21 | 1.008 | -1.32 ± 126.77i | 20.21 | 1.04 |
| | 0.35 ± 98.72i | 15.71 | 0.355 | -0.13 ± 97.25i | 15.49 | 0.76 |
| 40% | -0.12 ± 202.84i | 32.31 | 0.059 | -4.13 ± 214.56i | 34.22 | 1.92 |
| | -0.35 ± 160.51i | 25.62 | 0.218 | -1.73 ± 175.68i | 28.01 | 0.985 |
| | -10.34 ± 171.7i | 27.37 | 6.01 | -11.19 ± 175.09i | 27.85 | 6.39 |
| | -1.26 ± 126.93i | 20.21 | 0.992 | -1.32 ± 126.76i | 20.21 | 1.04 |
| | 0.35 ± 98.72i | 15.71 | 0.355 | -0.5 ± 97.26i | 15.49 | 0.514 |
| 50% | -0.12 ± 202.84i | 32.31 | 0.059 | -3.27 ± 215.05i | 34.22 | 1.52 |
| | -0.35 ± 160.5i | 25.62 | 0.218 | -1.68 ± 177.78i | 28.33 | 0.945 |
| | -10.03 ± 152.62i | 24.35 | 6.57 | -10.14 ± 153.4i | 24.51 | 6.61 |
| | -1.23 ± 126.93i | 20.21 | 0.969 | -1.32 ± 126.75i | 20.21 | 1.04 |

| | | | | | | |
|---|---|---|---|---|---|---|
| | 0.35 ± 98.72i | 15.71 | 0.355 | -0.6 ± 97.25i | 15.49 | 0.617 |
| 60% | -0.12 ± 202.84i | 32.31 | 0.059 | -2.92 ± 215.23i | 34.22 | 1.36 |
| | -0.35 ± 160.5i | 25.62 | 0.218 | -1.43 ± 177.94i | 28.33 | 0.804 |
| | -1.32 ± 126.93i | 20.21 | 1.04 | -1.38 ± 126.68i | 20.21 | 1.08 |
| | -9.95 ± 138.46i | 22.12 | 7.17 | -10.64 ± 138.96i | 22.12 | 7.63 |
| | 0.35 ± 98.72i | 15.71 | 0.355 | -0.41 ± 97.23i | 15.47 | 0.421 |
| 70% | -0.12 ± 202.84 | 32.31 | 0.059 | -2.92 ± 215.23i | 34.22 | 1.36 |
| | -0.35 ± 160.5i | 25.62 | 0.218 | -1.43 ± 177.94i | 28.33 | 0.804 |
| | 0.35 ± 98.72i | 15.71 | 0.355 | -0.41 ± 97.23i | 15.47 | 0.421 |
| | -1.32 ± 126.93i | 20.21 | 1.04 | -1.38 ± 126.68i | 20.21 | 1.08 |
| | -9.75 ± 127.39i | 20.37 | 7.63 | -10.64 ± 138.96i | 22.12 | 7.63 |
| 80% | -0.12 ± 202.84i | 32.31 | 0.059 | -2.92 ± 215.23i | 34.22 | 1.36 |
| | -0.35 ± 160.5i | 25.62 | 0.218 | -1.43 ± 177.94i | 28.33 | 0.804 |
| | -1.32 ± 126.93i | 20.21 | 1.04 | -1.38 ± 126.68i | 20.21 | 1.08 |
| | 0.35 ± 98.72i | 15.71 | 0.355 | -0.41 ± 97.23i | 15.47 | 0.421 |
| | -9.55+118.43i | 18.94 | 8.04 | -11.64 ± 138.96i | 22.12 | 8.37 |

*Table5.6: Eigenvalues of the test system with the designed PID controller, SSSC controller and TCSC controller with 40% series compensation.*

| Without controller | With PID controller | With SSSC controller | With TCSC controller |
|---|---|---|---|
| -0.36±298.16i | -0.37±298.16i | -1.85±298.17i | -1.8504±298.17i |
| -0.12±202.84i | -4.13±214.56i | -0.372±202.8i | -0.3526±202.82i |
| -0.35±160.51i | -9.19±175.09i | -0.128±160.2i | -0.5812±160.46i |
| -10.34±171.7i | -1.73±175.68i | -4.884±566.99i | -27.163±133.29i |
| -1.32±126.93i | -1.26±126.76i | -0.07±127.03i | -0.0315±127.01i |
| -0.35±98.72i | -0.05±97.26i | -0.235±98.908i | -0.0774±98.972i |
| 1.49±60.53i | -0.49±60.53i | -1.348±5.901i | -1.684±6.3i |

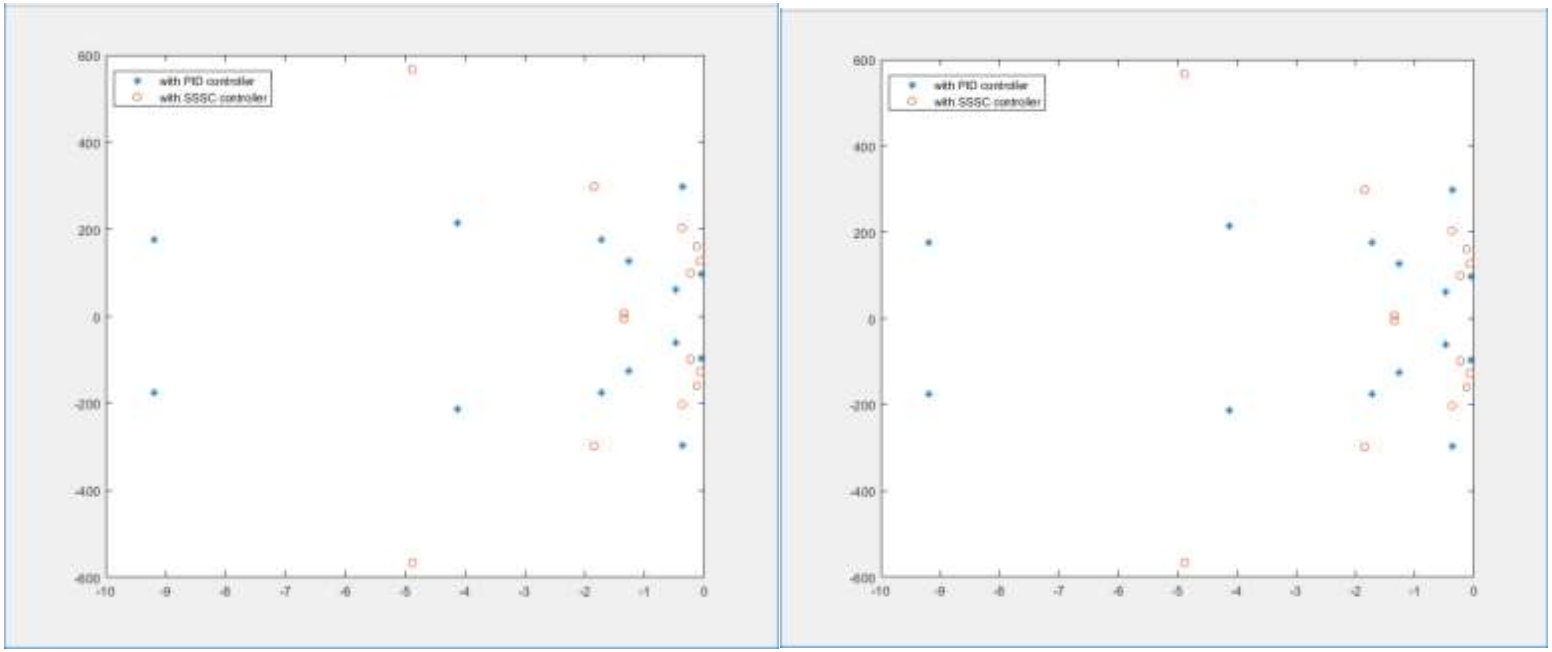


*Figure 5.1: Plotted eigenvalues of the test system with the designed PID controller, SSSC controller and TCSC controller with 40% series compensation.*

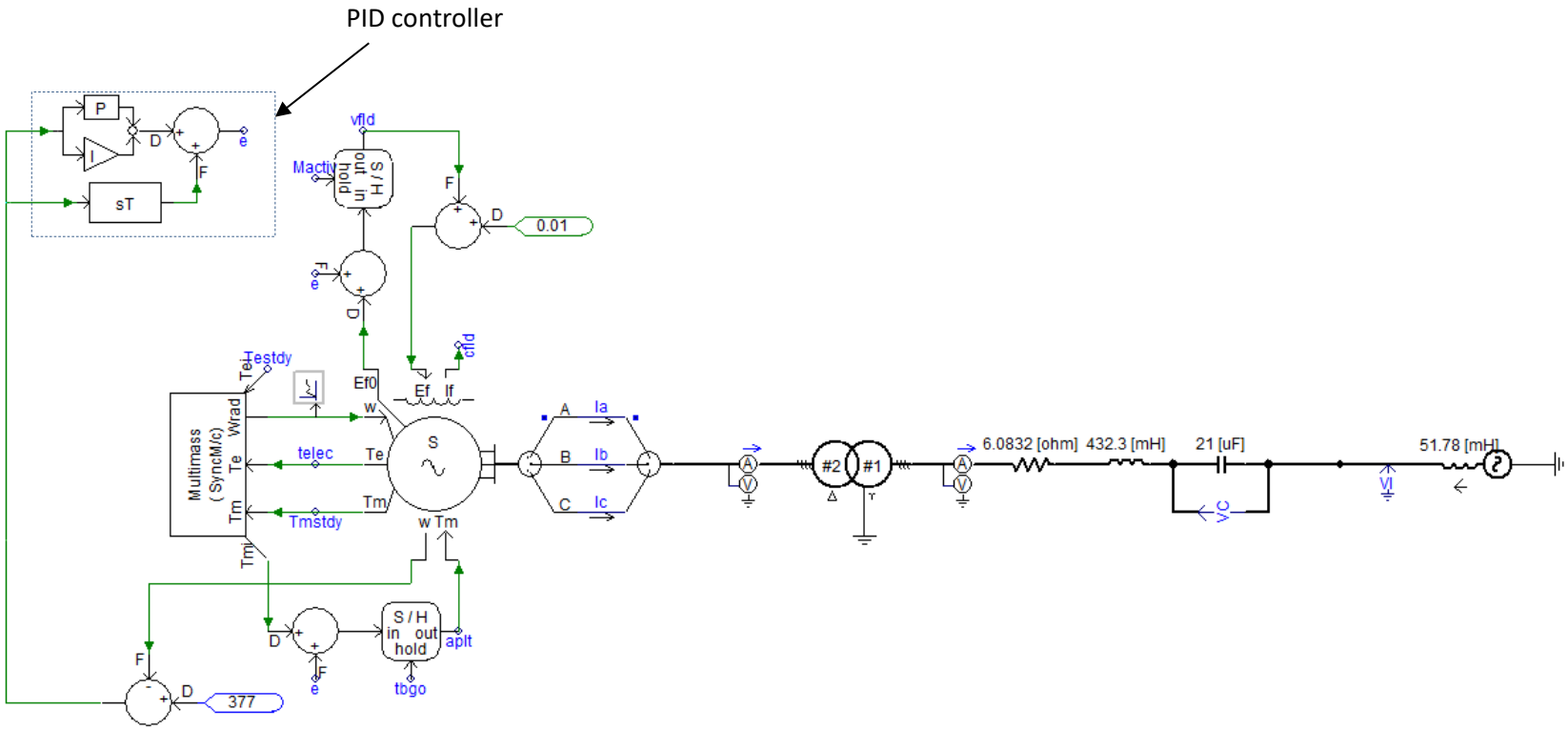


*Figure 5.2: Nonlinear PSCAD model with designed PID controller*

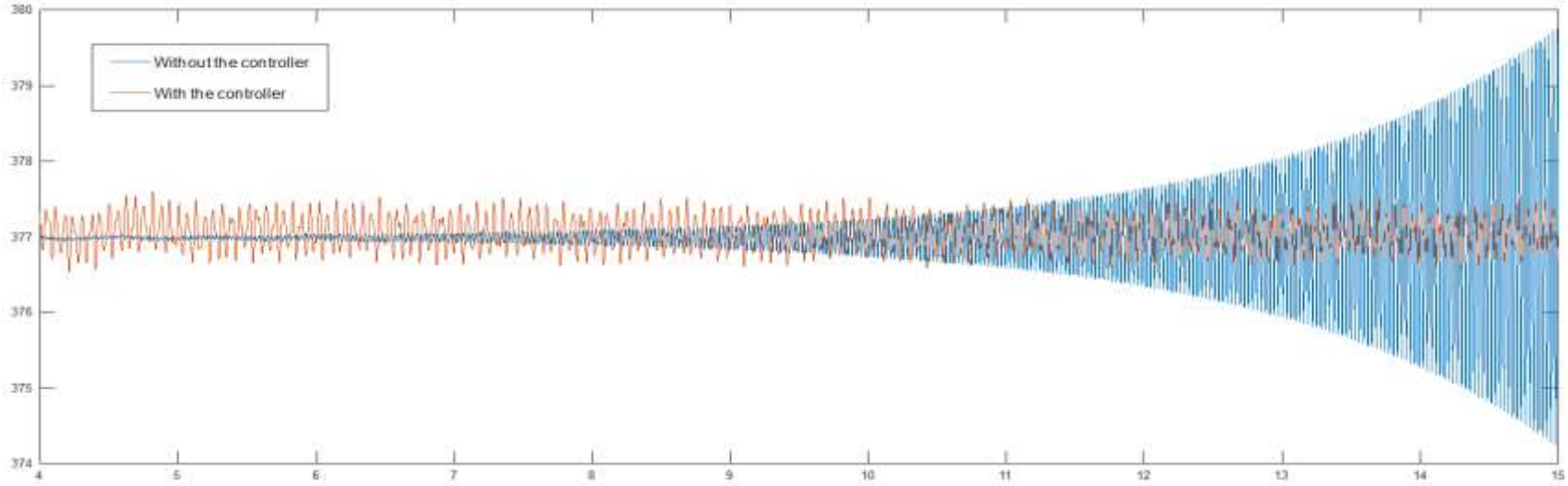


*Figure 5.3: Generator speed variation without and with the controller at 30% series compensation*

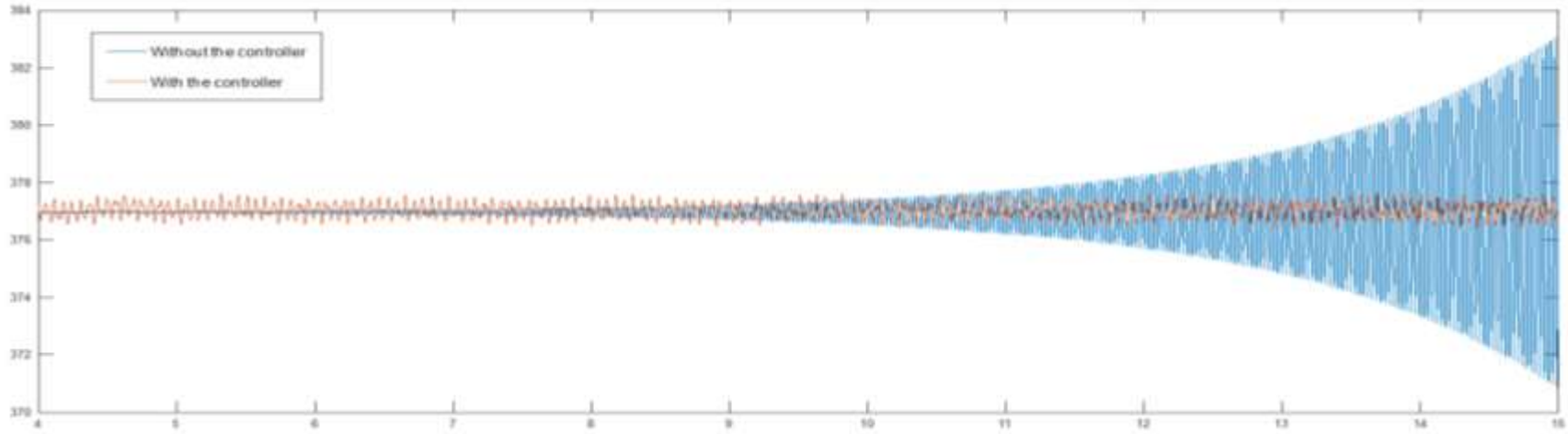


*Figure 5.4: Generator speed variation without and with the controller at 40% series compensation*

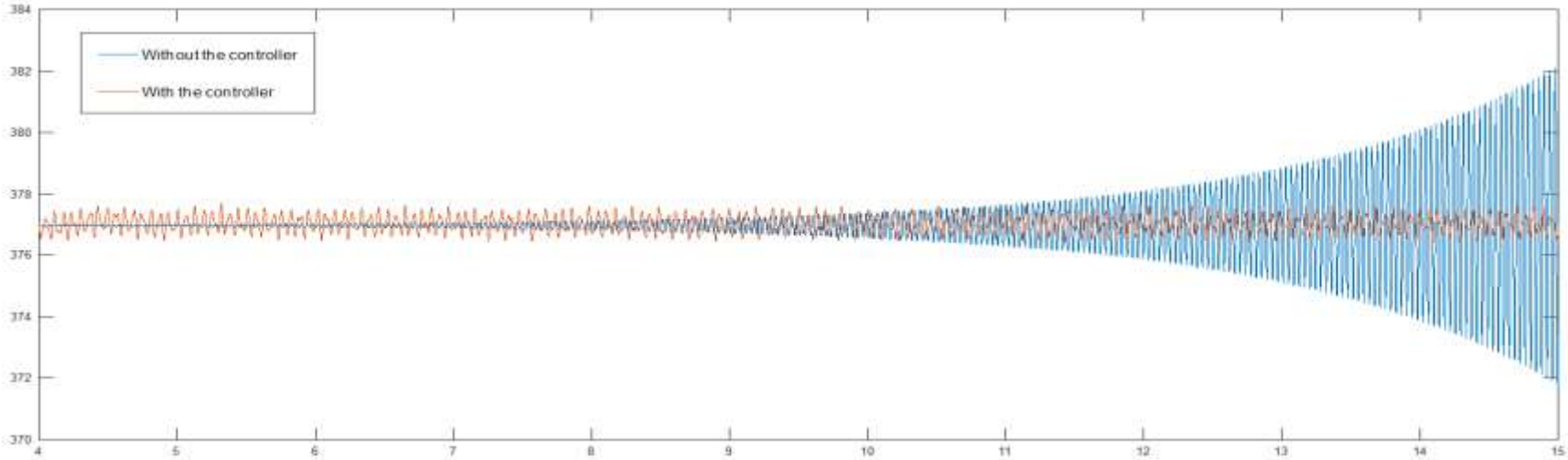


*Figure 5.5: Generator speed variation without and with the controller at 50% series compensation*

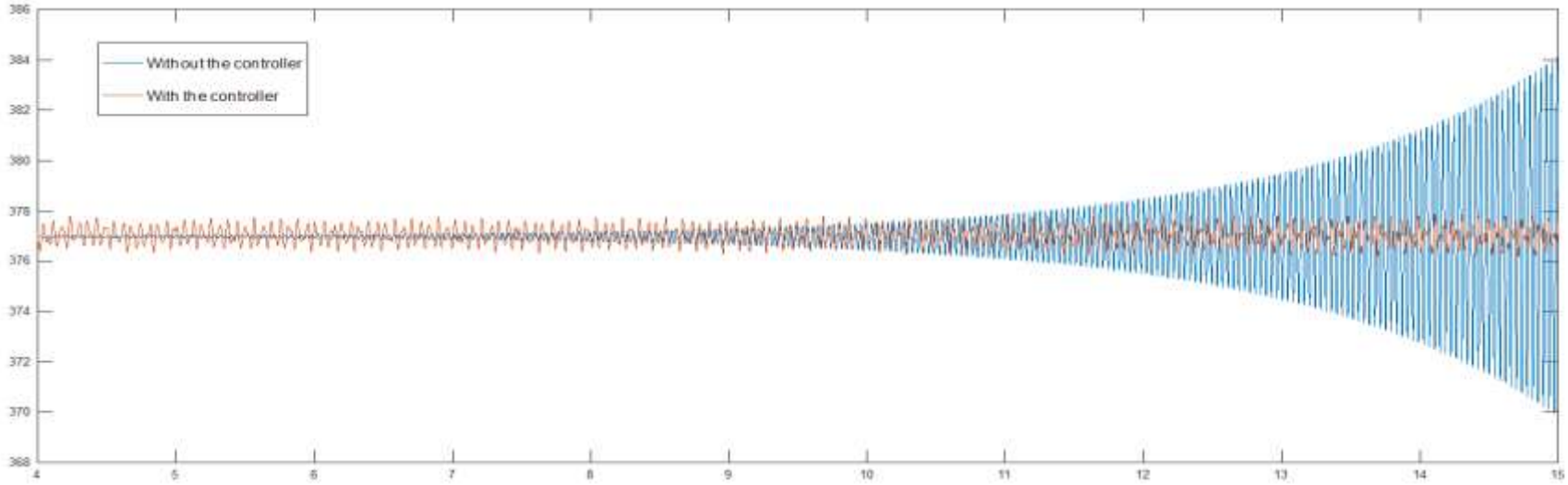


*Figure 5.6: Generator speed variation without and with the controller at 60% series compensation*

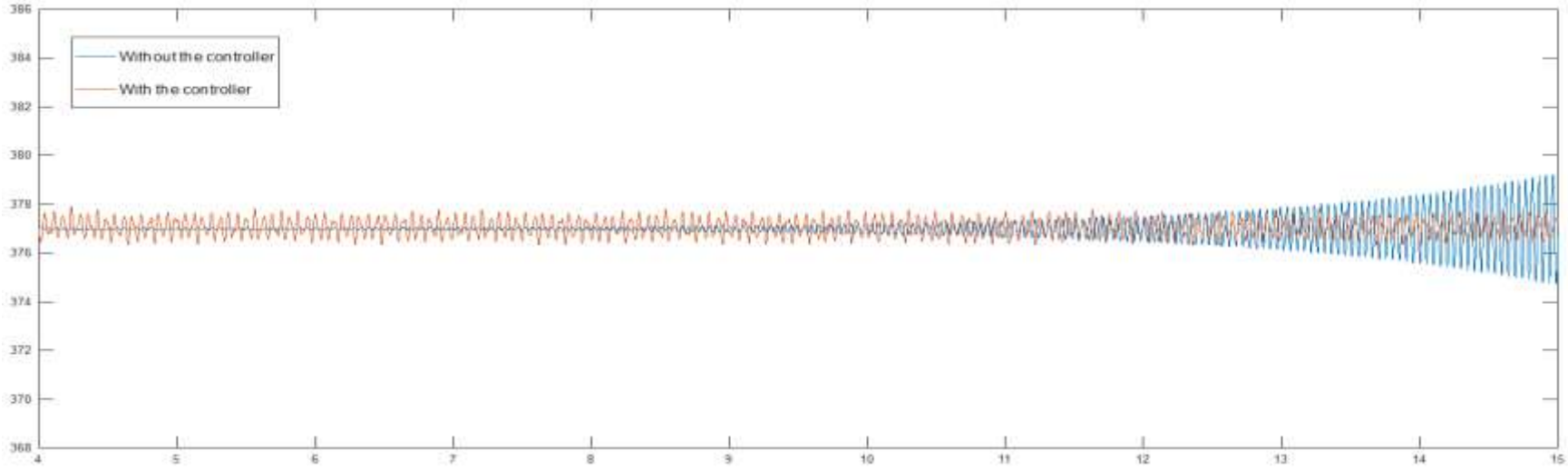


*Figure 5.7: Generator speed variation without and with the controller at 70% series compensation*

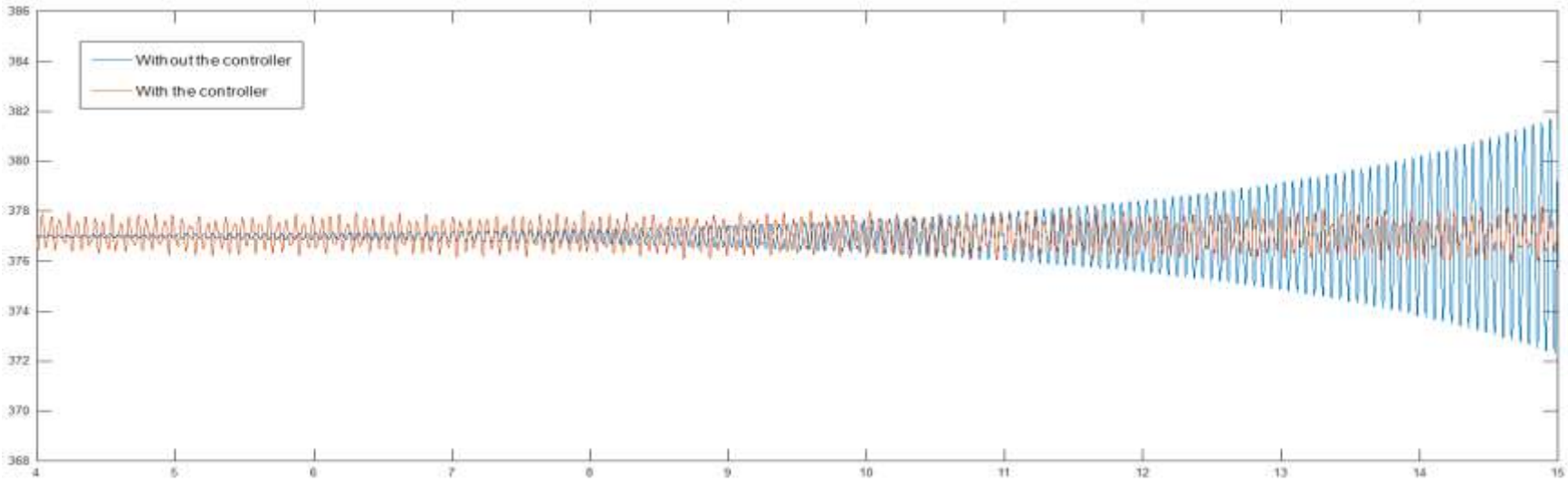


*Figure 5.8: Generator speed variation without and with the controller at 80% series compensation*

# CHAPTER 06

# CONCLUSION

Designing of a robust controller to damp sub-synchronous oscillations in power systems has been presented in this thesis. A PID controller was designed and simulated annealing method has been successfully applied to optimized the controller to perform well under different operating points of the selected power system. IEEE FBM was used to demonstrated the performance of the designed controller and the small signal model of the system was constructed using dynamic phasor approach. Performance of the controller designed in this study was demonstrated with the selected power system and the controller performs well with the different operating points of the system. the results are validated from the eigenvalues of the overall system as given in Table 5.5 and the speed variations of the generator (output waveforms) as shown in Figures 5.2 to 5.7.

## PUBLICATIONS

Gamage, C. M., & Wadduwage, D. P.. Designing a robust controller to damp sub-synchronous oscillations in power systems. 1–6. – accepted for MERCon 2020

## REFERENCES

[1] Zhu, W., Rajkumar, V., Spee, R., & Mohler, R. R. (1994). On the analysis of subsynchronous resonance in power systems. *Proceedings of the American Power Conference*, *56*(pt 1), 330–335.

[2] Paserba, J. (1997). Control of Power System Oscillations. *IFAC Proceedings Volumes*, *30*(17), 75–83. https://doi.org/10.1016/s1474-6670(17)46389-0

[3] Assi Obaid, Z., Cipcigan, L. M., & Muhssin, M. T. (2017). Power system oscillations and control: Classifications and PSSs' design methods: A review. *Renewable and Sustainable Energy Reviews*, *79*(January), 839–849. https://doi.org/10.1016/j.rser.2017.05.103

[4] Paserba, J., Sanchez-Gasca, J., Wang, L., Kundur, P. S., Larsen, E., & Concordia, C. (2017). Small-signal stability and power system oscillations. *Power System Stability and Control, Third Edition*, 10-1-10–23. https://doi.org/10.4324/b12113

[5] Villegas, H. N. (2011). *Electromechanical Oscillations in Hydro- Dominant Power Systems: An Application to the Colombian Power System*.

[6] Baker, D. H., Boukarim, G. E., D'Aquila, R., & Piwko, R. J. (2005). Subsynchronous resonance studies and mitigation methods for series capacitor applications. *Proceedings of the Inaugural IEEE PES 2005 Conference and Exposition in Africa*, *2005*(July), 386–392. https://doi.org/10.1109/pesafr.2005.1611851

[7] Chen, H., Guo, C., Xu, J., & Hou, P. (2013). Overview of Sub-synchronous Oscillation in Wind Power System. *Energy and Power Engineering*, *05*(04), 454–457. https://doi.org/10.4236/epe.2013.54b087

[8] Hosseini, S. H., & Mirshekar, O. (2001). Optimal control of SVC for subsynchronous resonance stability in typical power system. *IEEE International Symposium on Industrial Electronics*, *2*, 916–921. https://doi.org/10.1109/isie.2001.931593

[9] Suriyaarachchi, D. H. R., Annakkage, U. D., Karawita, C., Kell, D., Mendis, R., & Chopra, R. (2012). Application of an SVC to damp sub-synchronous interaction between wind farms and series compensated transmission lines. *IEEE Power and Energy Society General Meeting*, 1–6. https://doi.org/10.1109/PESGM.2012.6344797

[10] Prasad, C. E., & Vadhera, S. (2016). Fuzzy logic based SSSC as sub-synchronous resonance damping controller. *2015 International Conference on Energy, Power and Environment: Towards Sustainable Growth, ICEPE 2015*, 1–4. https://doi.org/10.1109/EPETSG.2015.7510175

[11] Rachananjali, K., Pavani, N., Suman, S., & Chaitanya, D. V. S. B. (2014). Damping of subsynchronous resonance using SSSC with hysteresis current control. *Proceeding of the IEEE International Conference on Green Computing, Communication and Electrical Engineering*, *ICGCCEE 2014*. https://doi.org/10.1109/ICGCCEE.2014.6922436

[12] Padiyar, K. R., & Prabhu, N. (2006). Design and performance evaluation of subsynchronous damping controller with STATCOM. *IEEE Transactions on Power Delivery*, *21*(3), 1398–1405. https://doi.org/10.1109/TPWRD.2005.861332

[13] El-Moursi, M. S., Bak-Jensen, B., & Abdel-Rahman, M. H. (2010). Novel STATCOM controller for mitigating SSR and damping power system oscillations in a series compensated wind park. *IEEE Transactions on Power Electronics*, *25*(2), 429–441. https://doi.org/10.1109/TPEL.2009.2026650

[14] Pilotto, L. A. S., Bianco, A., Long, W. F., & Edris, A. A. (2003). Impact of TCSC control methodologies on subsynchronous oscillations. *IEEE Transactions on Power Delivery*, *18*(1), 243–252. https://doi.org/10.1109/TPWRD.2002.803835

[15] Bhombe, R., & Nimje, A. (2013). *Sub - Synchronous Resonance Control Using Thyristor Controlled Series*. *2013*(Ratmig).

[16] Patel, C. (2015). *Simulation and Analysis of Sub-synchronous Resonance in a Series Compensated Transmission System*. 5(October), 1–10.

[17] Padiyar, K. R., & Prabhu, N. (2005). A comparative study of SSR characteristics of TCSC and SSSC. *15th Power Systems Computation Conference, PSCC 2005*, (January).

[18] Carlos E., & Ugalde-Loo (2010). Implementation Strategies for Corrective Control of Transmission Networks. *HVDC Doctoral Colloquium 2010,* (June).

[19] Arunprasanth S., Annakkage U.D., Karawita C., Kuffel R. Generalized Frequency Domain Controller Tuning Procedure for VSC Systems. *IEEE Transactions on Power Delivery 2015,* (June).

[20] Canizares, C., Fernandes, T., Geraldi, E., Gerin-Lajoie, L., Gibbard, M., Hiskens Tf Past Chair, I., … Vowles, D. (2017). Benchmark Models for the Analysis and Control of Small-Signal Oscillatory Dynamics in Power Systems. IEEE Transactions on Power Systems, 32(1), 715–722. https://doi.org/10.1109/TPWRS.2016.2561263